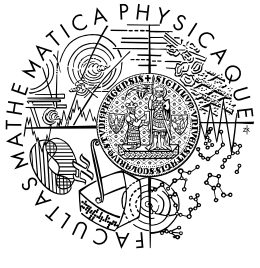

FACULTY
OF MATHEMATICS
AND PHYSICS
Charles University

HABILITATION THESIS

Ondřej Pejcha

Death of single and binary stars

Institute of Theoretical Physics

Prague 2021

Acknowledgement
I am grateful to my wife Eva, my daughters, and the rest of my family for their continuing understanding, tolerance, and patience. I thank my scientific colleagues and students who I have worked with and who influenced me over the years. In particular, I would like to thank my PhD advisor Todd Thompson, who taught me a great deal about being a theorist in astronomy and who continues to be a source of inspiration, and Brian Metzger, Kris Stanek, and Chris Kochanek for their friendship and mentoring.

My work at Princeton was supported by the NASA Hubble Postdoctoral Fellowship and Lyman Spizer Jr. Fellowship. At Charles University, my team has received support from the Primus Programme of Charles University, Czech Ministry of Education, Youth, and Sports, the European Research Council, and the Small Grants program of the US Embassy in Prague.

Introduction

This habilitation thesis is based on selected original papers published during my post-doctoral stay at the Department of Astrophysical Sciences, Princeton University, and my subsequent employment at the Institute of Theoretical Physics of the Faculty of Mathematics and Physics, Charles University. In all of these papers, I was either the first or second author.

The papers cover two related issues connected with the evolutionary endpoints of single and binary stars. In Chapter 1, I describe my work related to core-collapse supernovae, which mark the death of stars initially more massive than about 8 times the mass of our Sun. These bright events are observed over cosmological distances, leave behind neutron stars or black holes, and influence the formation of the next generation of stars by depositing newly-synthesized chemical elements as well as energy and momentum into the interstellar medium. My work covered in this thesis includes theoretical predictions of explosion properties, inferences of these properties from observed events, and the study of hydrodynamical interactions of core-collapse supernova explosions with pre-existing circumstellar material.

In Chapter 2, I present my work on a violent interaction phase experienced by some binary stars, the common envelope evolution. In this event, the two stars spiral in together and either survive with a significantly reduced orbit or merge into a single object. During the common envelope evolution the binary star loses considerable amount of mass, energy, and angular momentum. Common envelope evolution is a crucial ingredient of scenarios leading to close binary stars composed of at least one compact object (white dwarf, neutron star, or black hole). This includes binary black holes and binary neutron stars, where the common envelope evolution can bring the two compact objects sufficiently close together so that they later merge by gravitational wave emission. My work covered in this thesis has focused on the loss of mass from the binary leading up to the merger event and the associated implications for the observed transient brightenings. I also include a paper that argues for binary-influenced ejection of planetary nebula Sh 2-71 and a paper on characterization of stellar variability with the combination of time-domain photometric and spectroscopic surveys.

Each of these Chapters presents an overview of the topic including explanation of my contribution to the field, description of additional papers on the topic I co-authored, and a short perspective on future work. The overview does not have the ambition to provide a complete review of the field covering all of the open problems accompanied with a comprehensive set of references, but should be interpreted as a minimal description giving context to my work.

Contents

1 Death of single stars **5**
- 1.1 Overview . . . 5
  - 1.1.1 Collapse of the core and the subsequent explosion . . . 5
  - 1.1.2 Parameterized models of the neutrino mechanism . . . 7
  - 1.1.3 Light curves of normal hydrogen-rich core-collapse supernovae . . . 11
  - 1.1.4 Core-collapse supernovae with circumstellar interaction . . . 15
- 1.2 Additional co-authored works . . . 17
- 1.3 Future work . . . 18

2 Death of binary stars **19**
- 2.1 Overview . . . 19
  - 2.1.1 Stages of common envelope evolution . . . 20
  - 2.1.2 Hydrodynamics of L2 outflows . . . 22
  - 2.1.3 What powers luminous red novae? . . . 24
  - 2.1.4 Irregular shapes of planetary nebulae . . . 29
  - 2.1.5 Effects of binary evolution of stellar populations . . . 30
- 2.2 Additional co-authored works . . . 30
- 2.3 Future work . . . 31

Bibliography **33**

3 Original Papers **47**
- 3.1 Death of single stars . . . 47
  - 3.1.1 The landscape of the neutrino mechanism of core-collapse supernovae: neutron star and black hole mass functions, explosion energies, and nickel yields . . . 47
  - 3.1.2 A global model of the light curves and expansion velocities of Type II-Plateau supernovae . . . 47
  - 3.1.3 On the intrinsic diversity of Type II-Plateau supernovae . . . 47
  - 3.1.4 Supernova explosions interacting with aspherical circumstellar material: implications for light curves, spectral line profiles, and polarization . . . 47
- 3.2 Death of binary stars . . . 48
  - 3.2.1 Kinematics of mass-loss from the outer Lagrange point L2 . . . 48
  - 3.2.2 Cool and luminous transients from mass-losing binary stars . . . 48
  - 3.2.3 Binary stellar mergers with marginally bound ejecta: excretion discs, inflated envelopes, outflows, and their luminous transients . . . 48

3.2.4 Burying a binary: dynamical mass loss and a continuous optically thick outflow explain the candidate stellar merger V1309 Scorpii . . 48
3.2.5 Pre-explosion spiral mass loss of a binary star merger 48
3.2.6 Shock-powered light curves of luminous red novae as signatures of pre-dynamical mass-loss in stellar mergers 48
3.2.7 On the triple-star origin of the planetary nebula Sh 2-71 48
3.2.8 The ASAS-SN catalogue of variable stars – IV. Periodic variables in the APOGEE survey 49

Chapter 1

Death of single stars

1.1 Overview

Evolution of stars is driven by the loss of energy in the form of electromagnetic radiation or neutrinos. Stars compensate for these losses and maintain thermal equilibrium over long timescales by generating energy from nuclear burning in their cores. The quasi-steady nuclear burning stops either when the star cannot provide sufficient conditions to synthesize heavier atoms or when synthesizing heavier atoms would not yield additional energy. The evolution of solar-metallicity stars with initial masses smaller than about 8 masses of our Sun ($M_\odot$) ends with the formation of carbon-oxygen or oxygen-neon-magnesium core supported against its own gravity by the pressure of degenerate electrons – a white dwarf (WD). The core is surrounded by a hydrogen-rich envelope, which is eventually lost by strong stellar winds. As long as the flux of ionizing photons from the cooling WD is sufficient to ionize the lost envelope, we observe a planetary nebula. We will not discuss the evolutionary endpoints of low-mass stars in this Chapter any further.

Non-rotating solar-metallicity stars initially more massive than 8 $M_\odot$ evolve differently. Here, we leave aside the rare very massive stars that undergo (pulsational) pair instability (e.g. Woosley, 2017) or general relativistic instability (e.g. Chen et al., 2014) and instead we focus solely on massive stars with masses between about 8 and 100 $M_\odot$. These stars die with a collapse of the core, which leaves behind either a neutron star (NS) or a black hole (BH) and which can be sometimes observed as a bright supernova (SN).

1.1.1 Collapse of the core and the subsequent explosion

The cores of massive stars synthesize progressively heavier elements. After the ignition of carbon, the energy losses due to neutrino emission from the core become important and the core evolution timescale accelerates from thousands of years to mere hours and minutes. Ultimately, the star develops an inert electron-degenerate iron core, which grows in mass by nuclear burning in the overlying onion-like shells composed of progressively lighter elements (e.g. Woosley et al., 2002). Eventually, the iron core grows above the Chandrasekhar mass and cannot support itself against its own gravity anymore. The critical Chandrasekhar mass depends on the detailed chemical composition, residual thermal content of the core, general relativity corrections, and the pressure at the edge of the core. The core begins to collapse and the infall accelerates when the electron degeneracy support significantly reduces due to electrons combining with protons to form neutrons.

As the density increases, even neutrinos become trapped in the core. The collapse of the inner core halts when the density increases above the nuclear density and the hard-core repulsive component of the strong nuclear force becomes important.

At this point, the core bounces and forms a shock wave travelling outward through the supersonically infalling material. The shock wave does not propagate through the progenitor star, but instead stops its progress at 100–200 km from the center as it struggles to overcome the ram pressure of infalling material and energy losses due to neutrino cooling and photodisintegration of heavy nuclei passing through the shock. A quasi-static accretion phase ensues, which lasts hundreds of milliseconds to potentially more than a second. During this phase, the hot proto-neutron star (PNS) in the center is slowly contracting as its binding energy is carried away by neutrinos diffusing out through the dense layers. Neutrinos are also radiated from the infalling material, which accumulates on the PNS. A fraction of the radiated neutrinos, both those diffusing out of the PNS and those emitted from the accreting material, get absorbed below the accretion shock and cause neutrino heating.

It is currently believed that the combined effects of the neutrino heating, the associated convection and turbulence, and other instabilities like the standing accretion shock instability are successful in reviving the outward motion of the shock in a majority of stars. This is called the *neutrino mechanism*. If the shock revives, it propagates through the star and the resulting explosion is observed as a core-collapse supernova (CCSN). The CCSN rate in our Galaxy is approximately 0.01 to 0.03 yr^{-1} (Tammann et al., 1994; Adams et al., 2013).

The observed CCSN explosion is powered by the combination of the initial energy of the propagating shock, neutrino-driven wind from the PNS, recombination of protons, neutrons, and α particles to heavier atoms, and energy from explosive burning as the shock passes through the progenitor star. It is likely that multi-dimensional effects such as simultaneous accretion and explosion are important in powering the explosion (e.g. Müller et al., 2016). The fiducial asymptotic explosion energy of a neutrino-driven CCSN is $E_{\mathrm{exp}} \approx 10^{51}$ ergs although the observations suggest a considerable spread (Sec. 1.1.3). The binding energy of the NS is about 10^{53} ergs and is radiated away mostly in neutrinos, which implies relatively inefficient capture of neutrinos.

A successful CCSN leaves behind a NS. The mass of the NS is set by the mass of the core at bounce, which is set mostly by nuclear physics, and the accretion history, which varies greatly between different progenitor stars. Some NSs can later collapse to a BH either due to fall back of material that did not achieve escape velocity in the explosion or due to changes in the NS internal properties such as phase transitions or removal of rotation support. The maximum NS mass is set by the properties of the poorly-understood nuclear equation of state at high densities.

Successful CCSNe are also an important source of nucleosynthesis. As the shock propagates through the progenitor star, the post-shock gas is heated to high temperatures and undergoes nuclear burning to iron group elements. Another source of nucleosynthesis is the neutrino-driven wind from the PNS, where even heavier elements might be formed. Some of the newly synthesized elements are radioactive and the energy released in their decay powers certain phases of the optical emission of CCSNe. For example, the first few months of CCSNe are usually strongly influenced by the decay of ^{56}Ni. More details about CCSN light curves are discussed in Section 1.1.3.

In some stars, the stalled accretion shock does not revive its outward motion and the explosion fails. The shock retreats to the PNS, which eventually accretes enough mass to collapse to a BH. From the outside, the failed explosion might be accompanied by a transient significantly fainter than ordinary CCSN, which is caused by the reaction of the loosely-bound envelope to the sudden decrease of gravitational force as the NS binding energy escapes away in the form of neutrinos (Lovegrove and Woosley, 2013). In this case, the BH mass should be similar or higher than the helium-core mass, $M_{\rm BH} \gtrsim 6\,M_\odot$.

Establishing the viability of the neutrino mechanism of CCSNe has been a major unsolved problem of theoretical and computational astrophysics of the last 30 years. Investigations of the neutrino mechanism amalgamate multi-dimensional hydrodynamics coupled with neutrino physics and transport, high-density equation of state, nuclear reactions, and general relativity (e.g. Janka et al., 2016; Müller, 2020; Burrows and Vartanyan, 2021). Although rotation and magnetic fields are usually believed to be subdominant in ordinary massive star death, magnetorotational explosions are needed to explain some of the CCSN subtypes, which adds to the theoretical challenge. It is also worth noting that alternatives to the neutrino mechanism have been proposed. Some examples of include magnetorotational processes like jets or nuclear burning (e.g. Papish and Soker, 2011; Kushnir and Katz, 2015).

1.1.2 Parameterized models of the neutrino mechanism

The ultimate goal of CCSN explosion mechanism theory is to quantify the connection between the parameters describing massive stars (initial mass, metallicity, and rotation rate) and the outcomes of the core collapse (successful or failed explosion, properties of the compact remnant, explosion energy, yields of nuclei synthesized in the explosion). These predictions have to be confronted with observed CCSN populations. To achieve this goal, we need to employ a range of methods with various level of sophistication, because solving the full problem will be beyond our reach at least in the near future. Models with simplified physics are typically cheaper to run and usually introduce additional free parameters, which need to be calibrated by comparison with observations.

One specific model of the CCSN explosion mechanism is the framework of the *critical neutrino luminosity*, where the region between the stalled accretion shock and the PNS neutrinosphere is described as a spherically-symmetric steady-state accretion flow irradiated by neutrinos. This is a two-point boundary-value problem of ordinary differential equations, where the boundary conditions are the shock jump conditions at the outer boundary and a condition on neutrino optical depth at the inner boundary. The radius of the accretion shock is the eigenvalue of the problem. This model was first formulated by Burrows and Goshy (1993), who found that for a given mass-accretion rate through the shock ($\dot{M}$) there exists a critical neutrino luminosity emanating from the PNS ($L_{\nu,\rm crit}$) above which there are no steady-state solutions. The forbidden region of the parameter space is identified with explosions. The model is useful for quantitative studies of the importance of various physical effects on the neutrino mechanism. In a series of works, Yamasaki and Yamada (2005, 2006, 2007) studied the effects of rotation, convection, realistic equation of state, and the oscillatory stability. Pejcha et al. (2012a) explored the effect of collective neutrino oscillation on neutrino heating. Pejcha and Thompson (2012) examined the physics underlying $L_{\nu,\rm crit}$, quantified the dependence of $L_{\nu,\rm crit}$ on PNS mass and radius, neutrino energy, and accretion luminosity, and presented a new *antesonic* explosion condition equivalent to $L_{\nu,\rm crit}$.

In Pejcha and Thompson (2015), which is shown in full in Section 3.1.1, we have developed a parameterized model of CCSN based on $L_{\nu,\mathrm{crit}}$ that predicts whether a given progenitor star successfully explodes as a CCSN, what is the mass of the remnant NS, E_{exp}, and the amount of iron-group elements synthesized in the explosion. In this model, we take stellar structure of a range of progenitor stars and calculate long-term evolution of PNS mass, radius, and neutrino luminosity and energy using spherically-symmetric code GR1D (O'Connor and Ott, 2010). None of these calculations show explosions, as has been well-known for 1D SN simulations. We then assume that the evolution is quasi-static and compute the time sequence of $L_{\nu,\mathrm{crit}}$. Then, we artificially lower $L_{\nu,\mathrm{crit}}$ by an amount given by a simple power-law function with two free parameters and investigate whether the actual neutrino luminosity exceeds the modified explosion threshold. If this condition is satisfied, we assume that explosion was successful and estimate the explosion properties. We repeat this procedure for a large number of progenitor stars and different modifications of $L_{\nu,\mathrm{crit}}$ to explore the dependence of the observable outcomes on stellar structure and parameterization of the neutrino mechanism. We focus on two specific parameterization choices that yield: (a) approximately 25% fraction of failed explosions, or (b) all progenitors explode. The observable predictions for both parameterizations are shown in Figures 1.1, 1.2, and 1.3 and are discussed in more detail below.

A number of other works have addressed the same fundamental questions with different parameterized explosion models. Ugliano et al. (2012) used spherically-symmetric time-dependent simulations with simplified neutrino transport to study the dynamics from collapse to late explosion, to diagnose successful and failed explosions, and to estimate explosion energy and the amount of synthesized radioactive elements. PNS core was excised from the simulation and replaced with parametrically-contracting inner boundary. The parameters were calibrated on the observed properties of SN1987A. Ertl et al. (2016) revisited this model with updated physics and progenitor models and explored different calibrations based on SN1987A and observed CCSNe from stars near the lower limit of progenitor masses. Sukhbold et al. (2016) extended this model even further and provided detailed nucleosynthetic yields for many isotopes as well as SN light curves. Müller et al. (2016) simplified the problem to a system of ordinary differential equations and applied their model to a large number of progenitors. Perego et al. (2015), Curtis et al. (2019), and Ebinger et al. (2019, 2020) developed a different parameterization of spherically-symmetric CCSN dynamics and provided a wide range of observational predictions. Models of Mabanta et al. (2019) and Couch et al. (2020) implement simplified treatment of tubulence in spherically-symmetric simulations. Nakamura et al. (2015) explored dynamics of a large number of axisymmetric models.

While the results of most of these works differ in detail, there are common features that can be synthesized from this wide range of approaches. The most important result is that the core-collapse outcomes and CCSN properties are not a monotonic function of the initial mass of the star, but instead depend on the detailed structure of the innermost 2 to $3\,M_\odot$ of the progenitor. This is particularly striking in Figure 1.1, which shows outcomes for a range of initial progenitor masses at solar metallicity. The top panel shows the prediction found in many books dealing with stellar evolution: stars initially less massive than $25\,M_\odot$ leave behind NSs while more massive stars leave behind BHs (e.g. Carroll and Ostlie, 2007, p. 534). Often, it is implicitly assumed that all massive stars explode as CCSNe and the BHs are thus formed by fallback. The picture is quite different in the middle and bottom panels of Figure 1.1, where the successful and failed explosions are

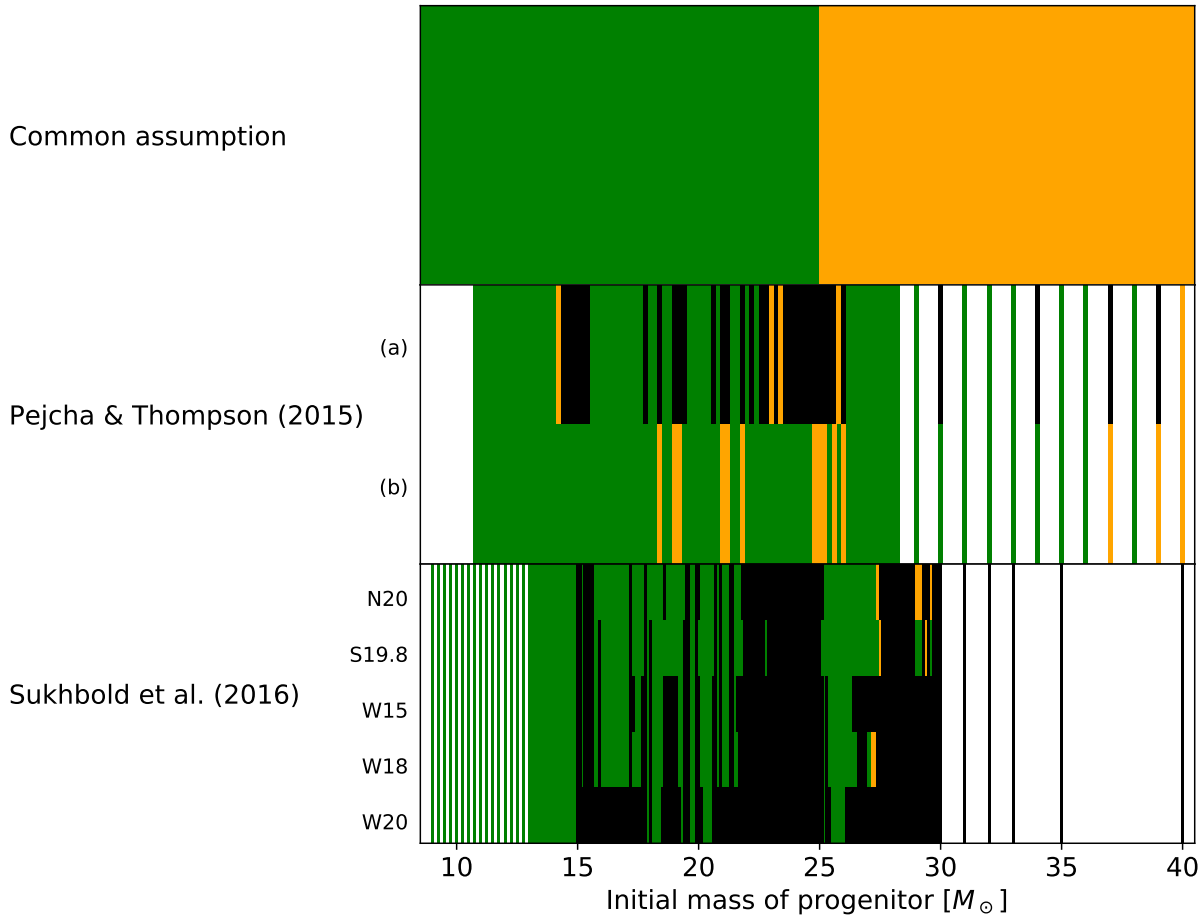

Figure 1.1: Mapping between the initial mass of a solar-metallicity star and the outcome of the collapse of the core: SN explosion leaving behind a NS (green), explosion with significant fall back leaving behind likely a BH (orange), and a collapse to a BH not accompanied by a traditional SN (black). The top panel shows the illustration of the common assumption that $25\,M_\odot$ is the dividing line between NS and BH formation (e.g. Carroll and Ostlie, 2007, p. 534). Middle panel shows the results of Pejcha and Thompson (2015) based on parameterized evolution of critical neutrino luminosity. In parameterization (a), there is a small but non-negligible fraction of direct collapse BHs, while in (b) all stars explode. Bottom panel shows results of hydrodynamical models of Sukhbold et al. (2016) for five different calibration models (N20, S19.8, W15, W18, W20). Middle and bottom panels show the complex landscape of core collapse outcomes that is a sensitive function of the internal core structure. All progenitors are shown with bars of constant width; white spaces corresponds to initial masses with no calculated progenitors. More complete comparison of theoretical predictions is discussed by Pejcha (2020).

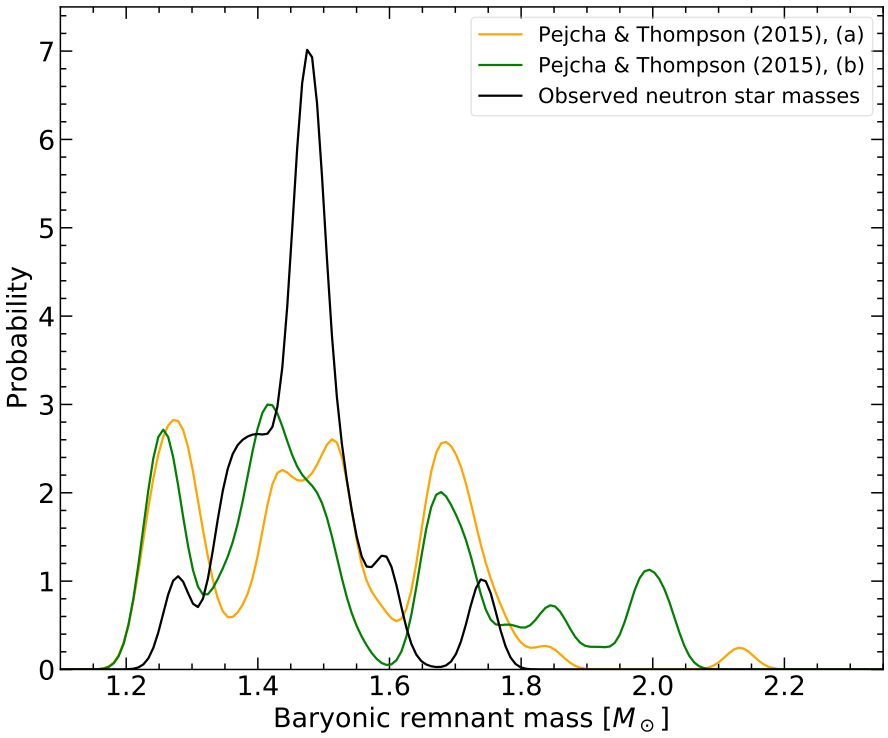

Figure 1.2: Distribution of birth masses of NSs. Orange and blue lines are based on theoretical predictions of Pejcha and Thompson (2015) for two different parameterizations of the neutrino mechanism and assuming single stars formed with Salpeter (1955) initial mass function. Black line shows the distribution of masses of double NSs and non-recycled pulsars based on the compilation of Özel and Freire (2016). All values are smoothed with a Gaussian kernel and converted to baryonic mass (without taking into account the binding energy) using relation of Timmes et al. (1996).

mixed in a complex pattern and not a simple monotonic function of the initial progenitor mass. For the considered progenitors, there are "islands" of BH formation around 15 $M_\odot$ and 20–25 $M_\odot$.

This pattern of explodability is reasonably well reproduced by a simple quantity describing the structure of the pre-collapse core, the *compactness* (O'Connor and Ott, 2011). Compactness is defined as a ratio of enclosed mass and its corresponding radius, which are evaluated just before the core collapse begins. Compactness is typically computed for enclosed masses between 1.5 and 3 $M_\odot$, which corresponds to progenitor layers that most strongly influence the core-collapse outcome. Alternatively, compactness is evaluated at specific values of entropy or electron fraction, which help to distinguish between layers of different composition. Progenitor dependence of the compactness as well as the rugged landscape of CCSN explosions shown in Figure 1.1 can be explained by the sensitivity of late stages of stellar evolution, especially nuclear burning in multiple shells, to initial conditions (e.g. Sukhbold and Woosley, 2014; Sukhbold et al., 2018).

One distinct prediction of the explosion landscape from Figure 1.1 is that most stars either successfully explode and leave behind a NS or fail to explode and should mostly collapse to a BH. This feature naturally explains the BH mass gap, which has been claimed to exist between about 2 and 5 $M_\odot$ (e.g. Özel et al., 2010). It has been unclear whether

this feature is a true gap with no objects or a region of parameter space with fewer objects (e.g. Kreidberg et al., 2012; Ertl et al., 2020). Probing the existence and properties of this mass gap is an important goal of gravitational wave interferometers. Simultaneously, there has been an independent effort to identify BHs possibly lying in the gap (e.g. Thompson et al., 2019; Rivinius et al., 2020; Jayasinghe et al., 2021b; Masuda and Hirano, 2021; Gomel et al., 2021).

Another prediction of the parameterized models is the detailed distribution of NS masses. In Figure 1.2, we show results from Pejcha and Thompson (2015) along with the observed distribution compiled by Özel and Freire (2016). The observed distribution is based on modeling general-relativistic effects in radio observations of NS binaries containing at least one pulsar. Most of the measurements come from double NS binaries, where both components have masses approximately close to their birth mass. The rest comes from non-recycled pulsars with WD companions. In most cases, the mass measurements are very precise and were intentionally smoothed for the purposes of this plot. A number of works have tried to quantitatively compare theoretical and observed NS mass distributions (e.g. Pejcha et al., 2012b; Raithel et al., 2018). Typically, there are disagreements in the relative frequency of low-mass ($M_{\rm NS} \approx 1.4\,M_\odot$) and high-mass ($M_{\rm NS} \approx 1.7\,M_\odot$) NSs. It is likely that the preceding binary evolution led to a different distribution of core properties than expected from single-star evolution (e.g. Ertl et al., 2020; Patton and Sukhbold, 2020; Woosley et al., 2020).

In Figure 1.3, we illustrate the predictions of Pejcha and Thompson (2015) for explosion energy $E_{\rm exp}$, ejecta mass $M_{\rm ej}$, and the amount of radioactive nickel synthesized in the explosion $M_{\rm Ni}$. The theoretical results show a relatively tight correlation between $E_{\rm exp}$ and $M_{\rm Ni}$, which is explained by more energetic SNe exposing larger amount of material to high-enough temperatures to synthesize ^{56}Ni. The scatter in the correlation is due to differences in the detailed structure between individual progenitors. There is no strong predicted correlation between $M_{\rm ej}$ and $E_{\rm exp}$, which is surprising, because there is a belief that more massive stars should yield more energetic CCSNe. Other parameterized CCSN models show similarly weak correlation between these two quantities (Pejcha, 2020). The observed values of these quantities are described in more detail in the next Section.

Finally, it is important to remark that the results from parameterized models have to be interpreted carefully. The specific choice of the parameterization constrains the range of the outcomes, which can become too reduced. For example, if one were to relate the additional neutrino heating to the compactness of the progenitor, then finding trends of observables with respect to compactness might not be entirely surprising. For this reason, full 3D models are indispensable in revealing the important trends and outcomes. Indeed, some of the recent works point against the correlation of the explosion properties with the compactness (Burrows et al., 2020).

1.1.3 Light curves of normal hydrogen-rich core-collapse supernovae

Theories of CCSN explosions ought to be confronted with observations. Out of the large number of possible observations, it is tempting to utilize as much as possible optical observations of CCSNe. These observations are regularly secured for events in a much larger volume than what is possible with direct detections of neutrinos or gravitational waves with current technology. Thanks to new generations of science surveys, the number

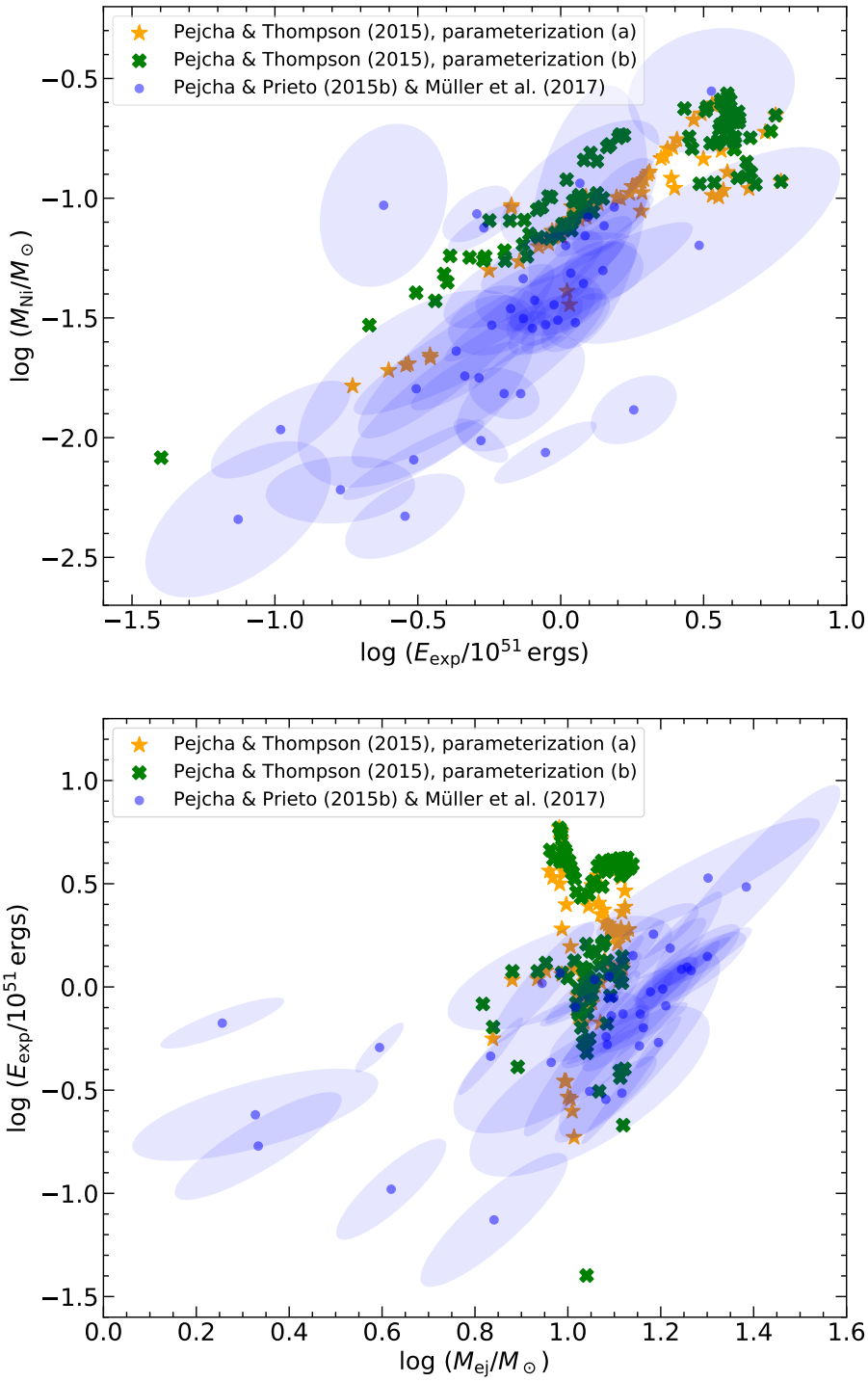

Figure 1.3: Explosion energy $E_{\rm exp}$, ejecta mass $M_{\rm ej}$, and the mass of radioactive nickel $M_{\rm Ni}$ of CCSN explosions. Green crosses and orange stars show theoretical predictions of Pejcha and Thompson (2015), while the blue dots show inferences from observations using combined results from Pejcha and Prieto (2015b) and Müller et al. (2017). Blue ellipsoids show 1σ uncertainty taking into account the covariance between the inferred quantities.

of CCSNe discovered every year has been steadily growing and should reach $\gtrsim 10^5$ per year once the Vera C. Rubin Observatory (previously known as Large Synoptic Survey Telescope) commences regular observations in 2023 (LSST Science Collaboration, 2009). Turning this accelerating growth of available data into useful statements on the CCSN explosion mechanism is a challenge.

Not all SN types are equally useful for constraining the explosion mechanism. SNe are classified based on their optical spectra and light curves as hydrogen-poor (Type I) or hydrogen-rich (Type II) (e.g. Filippenko, 1997). Type I SNe are further subdivided based on the presence of silicon lines (Ia), helium lines (Ib), or absence of both (Ic). Type Ia SNe are associated with thermonuclear events on white dwarfs and are not related to massive stars. Progenitors of Type Ib and Ic SNe are likely massive stars with their hydrogen and helium envelope layers removed either due to intense stellar winds or interactions in binary stars. Type II SNe are commonly associated with massive stars that were able to preserve most of their hydrogen envelopes and are further subdivided based on their light curve showing either plateau (IIP) or linear decline (IIL). Although Type IIP and IIL SNe are in many aspects similar, the theoretical explanation for the linear decline in Type IIL SNe is not yet clear (Anderson et al., 2014; Faran et al., 2014; Valenti et al., 2015; Morozova et al., 2017; Arcavi, 2017). Additional subtypes are Type IIb SNe with only thin hydrogen envelope and Type IIn SNe with narrow emission lines indicating presence of a shock interaction between the SN ejecta and surrounding dense medium. Observational efforts have also identified a number of SNe that posses qualities of two or more classes or are peculiar in other ways. Type IIP SNe are the best choice for comparison with CCSN explosion models, because their progenitors are the least affected by binary interactions or other unsolved massive star mysteries.

We now focus on understanding the light curves of Type IIP SNe. A few days after the SN shock travels through the progenitor star, the kinetic energy of the ejecta dominates over the thermal energy. Subsequently, the ejecta expands nearly homologously so that mass shells are ordered by their velocity and the radius of each shell increases linearly with time. The evolution of the ejecta energy and its internal distribution depend on the diffusion of radiation within and out of the ejecta, adiabatic losses, complications in the equation of state and opacities due to ionization/recombination, and additional heating such as the decay of radioactive elements or energy input from a central compact object.

The first light signature of a Type IIP SN is a shock breakout emission when the radiation trapped behind the shock diffuses ahead and leaves. The duration of this UV or X-ray emission spike is of the order of light-crossing time of the progenitor, which makes it hard to detect. The outer layers of the shocked envelope then continue to cool for a few hours or days. After that, the light curve exhibits a phase of nearly constant bolometric luminosity, the *plateau*, which typically lasts $t_{\rm pl} \approx 100\,{\rm days}$. During this period, the light diffuses out of the ionized part of ejecta with a relatively sharp edge set by the hydrogen recombination front. The observed plateau luminosity $L_{\rm pl}$ spans a relatively wide range from about $10^{41}\,{\rm erg\,s^{-1}}$ to few times $10^{42}\,{\rm erg\,s^{-1}}$. The plateau is followed by a drop in luminosity, which happens when all of the hydrogen recombines and becomes nearly transparent. Subsequently, the light curve follows an exponential decline powered by thermalization of radioactive decay products, where the ^{56}Ni chain is dominant in the first few hundreds of days.

The distinct observed features of Type IIP SN light curves directly depend on physical parameters relevant for the CCSN explosion. The luminosity and duration of the plateau

depend on $E_{\rm exp}$, $M_{\rm ej}$, and the initial progenitor radius R_0. Adding spectroscopically-determined expansion velocity of the photosphere, $v_{\rm ej} \approx \sqrt{E_{\rm exp}/M_{\rm ej}}$, we have three observables ($L_{\rm pl}$, $t_{\rm pl}$, $v_{\rm ej}$) for three unknown physical quantities ($E_{\rm exp}$, $M_{\rm ej}$, R_0). These sets of quantities are tied together by analytic power-law scaling relations (Litvinova and Nadezhin, 1985; Popov, 1993), which have been calibrated using radiation hydrodynamics (e.g. Kasen and Woosley, 2009; Sukhbold et al., 2016). If we assume complete trapping and thermalization of radioactive decay products, the luminosity during the exponential decay is directly proportional to $M_{\rm Ni}$. Additional extra heating by ^{56}Ni decay slightly extends and brightens the plateau, which can be taken into account in the analytic relations.

Practical implementation of the inversion $(L_{\rm pl}, t_{\rm pl}, v_{\rm ej}) \rightarrow (E_{\rm exp}, M_{\rm ej}, R_0)$ has faced a number of problems. First, it is difficult to assemble the necessary observations. Type IIP SNe are relatively faint, which is exacerbated by the luminosity drop after the plateau ends. The light curve typically has to be followed over $\gtrsim 200$ days, which is complicated by the changing position of the Sun. Ideally, simultaneous observations spanning near-ultraviolet to near-infrared should be secured to reliably reconstruct the bolometric light curve. Although only low-resolution spectra are required to measure $v_{\rm ej}$, these observations are more costly than photometry.

Second, it is necessary to know the time of explosion as precisely as possible and to have reliable estimates of the distance and extinction to the SN. Fortunately, for Type IIP SNe these parameters can be constrained with the observations of the SN using the expanding photosphere method (e.g. Kirshner and Kwan, 1974), but at the price of introducing additional free parameters. Uncertainties in these additional degrees of freedom propagate to the estimates of physical explosion parameters.

Third, it is not completely clear how to infer the required quantities from the observed features. For example, transition from the plateau to the exponential decay can last few days or more, which makes $t_{\rm pl}$ uncertain. Similarly, $L_{\rm pl}$ is not strictly constant during the plateau. Analogous obstacles are encountered when comparing the entire set of observations to synthetic observations based on radiation hydrodynamics calculations. In this case, the imperfect treatment of radiation transport and incomplete knowledge of microphysical quantities like opacities preclude matching theory to observations within the observational uncertainties. The modeling outcome is then systematically biased depending on which part of the data is fitted and how are the observations distributed.

Finally, inferences of some physical quantities might be significantly correlated or even completely degenerate. For example, increasing $E_{\rm exp}$ while keeping $M_{\rm ej}$ constant leads to faster expansion of the ejecta and faster diffusion of the light. $M_{\rm ej}$ can be increased to compensate and if $v_{\rm ej}^2 \approx E_{\rm exp}/M_{\rm ej}$ stays roughly constant, our ability to infer $E_{\rm exp}$ and $M_{\rm ej}$ independently is limited (e.g. Nagy et al., 2014; Pejcha and Prieto, 2015b; Goldberg et al., 2019; Goldberg and Bildsten, 2020; Dessart and Hillier, 2019). These inherent physical degeneracies necessitate proper statistical treatment of the inferred quantities.

We have developed in Pejcha and Prieto (2015a), which is shown in full in Section 3.1.2, a global model of Type IIP light curves and expansion velocities, which aims to address the issues described above. The plateau phase of each SN is phenomenologically modeled by its time evolution of radius and effective temperature. The radioactive decay tail is described by an exponential with free normalization and timescale. These quantities are transformed to multi-band light curves and expansion velocity curves using a polynomial mapping, where the coefficients are fitted from the data by making use of the similarity

between different events. This formulation leads to a global optimization problem, where each SN is described by a set of "local" quantities (distance, extinction, light curve parameters, etc.) and where the "global" parameters (coefficients of polynomial mapping) are the same for all events. We trained the model on a sample of nearby well-observed SNe. Taking into account uncertainties and covariances between model parameters, we derived a consistent set of quantities like relative distances, extinctions, spectral energy distribution evolution sequences, bolometric corrections, and dilution factors without any need for theoretical atmosphere models.

In Pejcha and Prieto (2015b), which is shown in full in Section 3.1.3, we applied the model to derive the physical quantities of interest for CCSN explosion models ($E_{\rm exp}$, $M_{\rm ej}$, R_0, $M_{\rm Ni}$) using analytic scaling relations of Litvinova and Nadezhin (1985) and Popov (1993). The inferred values are shown in Figure 1.3. We quantified the covariance between these parameters and found that it can be significant for certain parameter combinations. For example, the covariance between $L_{\rm pl}$, $E_{\rm exp}$, and $M_{\rm Ni}$ is dominated by the uncertainty in the distance, which leads to additional spread closely aligned with the physical correlation between these two quantities. Similarly, the degeneracy in the inferences of $E_{\rm exp}$ and $M_{\rm ej}$ casts doubt on whether this correlation important for theory actually exists in the observed events.

There have been a number of works with estimates of Type IIP SN explosion parameters from light curves and spectroscopic expansion velocities. One of the first looks at physical parameters was done by Hamuy (2003) who used the same analytic scaling relations as we did. Works based on radiation hydrodynamics often employ the flux-limited diffusion approximation in spherical symmetry (Pumo et al., 2017; Morozova et al., 2018; Utrobin and Chugai, 2019; Eldridge et al., 2019). These analyses have not generally provided mutually consistent results compatible with other methods like direct progenitor detections. To summarize, the $E_{\rm exp}$–$M_{\rm Ni}$ correlation seems robust and physical, while more work is needed to characterize the relation between $E_{\rm exp}$ and $M_{\rm ej}$. The fundamental issue of degeneracy between certain parameters can be addressed with additional observations, although sometimes quite challenging to obtain. For example, very early data in the shock breakout or shock cooling phase of the light curve can yield constraints on R_0 (e.g. Yaron et al., 2017; Goldberg et al., 2019). Another example is the nebular-phase spectroscopy of the oxygen lines, which can constrain $M_{\rm ej}$ (e.g. Silverman et al., 2017; Dessart and Hillier, 2020).

1.1.4 Core-collapse supernovae with circumstellar interaction

CCSN light curves can be affected by a number of additional effects. A particularly striking complication is a collision between the SN ejecta and a dense circumstellar medium (CSM). The resulting radiative shock can thermalize a significant fraction of the kinetic energy of the SN ejecta, which can power a much brighter transient than the original SN. In order to achieve an efficient conversion, a sufficiently dense CSM needs to be located relatively close to the progenitor. It is unclear how and why such CSM could arise and how it is connected to poorly-understood final evolutionary phases of massive stars, their instabilities, and their binary nature.

A valuable insight into the origin of the CSM can come from its spatial distribution. Although spherical symmetry is often assumed for the CSM, relaxing this assumption can give rise to distinct new phenomena. For example, CSM shaped in the form of a narrow

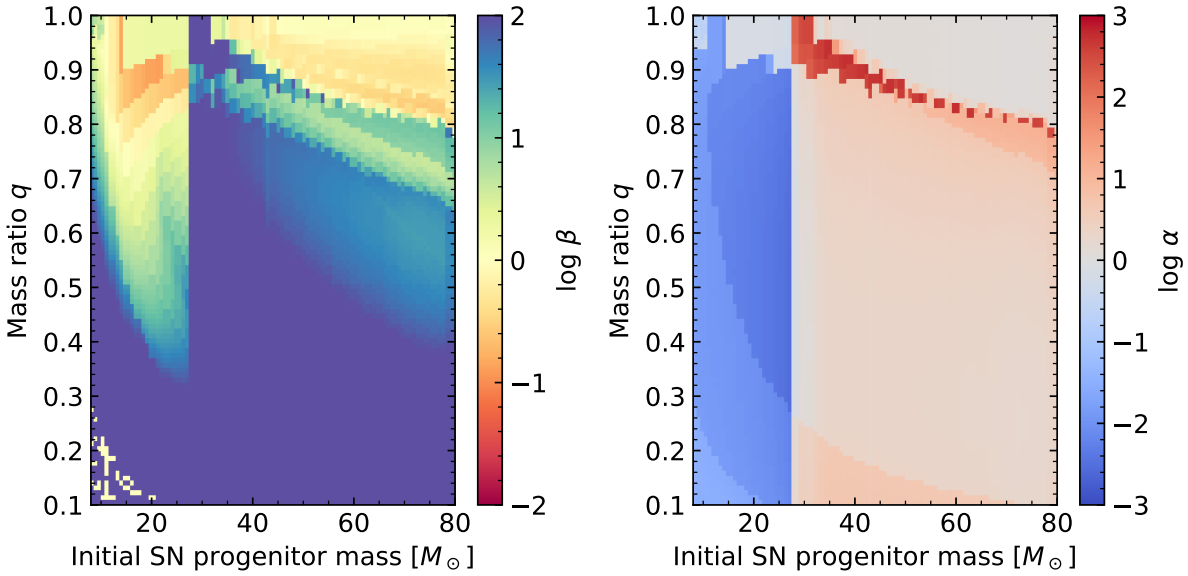

Figure 1.4: Colliding wind properties for binary stars at the moment when the more massive star explodes as a SN as a function of the initial mass of the progenitor and the binary mass ratio at birth. Binary star orbit is assumed sufficiently wide so that no mass transfer has occurred. We show the ratio of wind momenta β (left panel) and wind velocities α (right panel). The quantities are obtained by combining assumptions on wind terminal velocities with single-star evolution tracks from BPASS v2.2.1 (Eldridge et al., 2017; Stanway and Eldridge, 2018).

disk confines the shock interaction into a ring and the remaining part of the SN ejecta expands and radiates freely. In some cases, the freely expanding ejecta might engulf the shock interaction region and make it effectively work as an internal power source re-energizing the ejecta (e.g. Mauerhan et al., 2013b; Smith, 2013, 2017; Andrews and Smith, 2018; Margutti et al., 2019). Disk-like CSM distributions are naturally associated with mass ejection from binary stars, where the orbital plane is the preferred region of matter accummulation. Interacting SNe with disk-like CSM have been investigated with a range of approaches in (radiation) hydrodynamics (Vlasis et al., 2016; McDowell et al., 2018; Suzuki et al., 2019; Kurfürst and Krtička, 2019). This type of CSM of interaction is of potential importance in other types of stellar explosions associated with binary stars like classical novae (e.g. Chomiuk et al., 2014, 2020; Li et al., 2017; Aydi et al., 2020) or luminous red novae (Sec. 2.1.3).

A less explored aspherical CSM geometry is a shell formed in the collision of two powerful winds in a binary star. Since binary stars are relatively frequent among massive stars, this CSM should be commonly present. In Figure 1.4, we show the basic properties of colliding wind shells for binary stars at the moment when the first star explodes as a CCSN. The binary orbit is sufficiently wide so that both stars evolve as effectively single. We show the ratio of wind momenta $\beta = (\dot{M}_{\mathrm{w},A} v_{\mathrm{w},A})/(\dot{M}_{\mathrm{w},B} v_{\mathrm{w},B})$ and wind velocities $\alpha = v_{\mathrm{w},A}/v_{\mathrm{w},B}$, where $\dot{M}_{\mathrm{w}}$ and v_{w} are wind mass-loss rates and terminal velocities of binary components A and B. We see that binaries composed of red supergiants and hotter main sequence stars can have $\beta \approx 1$. Kochanek (2019) argued that colliding wind shells in such binaries could explain the "flash-ionization" signature seen in very early

spectra a some CCSNe. However, effect of colliding wind shells on light curves has not been sufficiently explored so far.

In Kurfürst et al. (2020), which is shown in full in Section 3.1.4, we performed hydrodynamic simulations of a spherical SNa ejecta colliding with various axisymmetric CSM distributions with the aim of finding out whether different CSM distributions provide uniquely defined signatures. We considered a disk, various types of colliding wind shells, and a bipolar nebula modeled after η Car. We found that the CSM–SN collision layer is composed of normal and oblique shocks, reflected waves, and other hydrodynamical phenomena that lead to various instabilities. We post-processed the hydrodynamic simulations to obtain approximate light curves under the assumption that shock heating is fully reprocessed by the SN ejecta, distribution of line-of-sight velocities that approximate line profiles at late times, and estimates of polarization signatures. One notable result is that colliding wind shell CSM leads to asymmetric and time-evolving line profiles, which could explain some of the mysterious observed events (e.g. Smith et al., 2015; Bilinski et al., 2020).

1.2 Additional co-authored works

- **Holoien et al. (2016)**

  Analysis of an unusually luminous Type II SN, which makes use of the light curve fitting models of Pejcha and Prieto (2015a) (Sec. 3.1.2).

- **Müller et al. (2017)**

  Extension of the work of Pejcha and Prieto (2015b) (Sec. 3.1.3), which essentially doubles the sample of objects and focuses specifically on comparing the inferred nickel masses with theoretical predictions.

- **Raives et al. (2018)**

  This work extends the polytropic formulation of $L_{\nu,\mathrm{crit}}$ of (Pejcha and Thompson, 2012) to time-dependent solutions and investigates transition from the accretion to explosion phases.

- **Szalai et al. (2019a)**

  A detailed analysis of Type IIP SN SN2017eaw, which makes use of the light curve fitting tool of Pejcha and Prieto (2015a).

- **Szalai et al. (2019b)**

  Unified analysis of infrared photometry of SNe of all kinds from *Spitzer* space telescope. For several SNe, the light curve fitting tool of Pejcha and Prieto (2015a) was used.

- **Pejcha (2020)**

  Book chapter, which reviews the status of parameterized CCSN explosion models, their predictions of observables, and compares them to inferences made from CCSN light curves and spectra.

1.3 Future work

The field of CCSNe is moving rapidly forward both in theory and observation. The theoretical frontier of the neutrino mechanism of CCSN explosions has moved to 3D simulations with sophisticated neutrino transport. Developing the necessary tools requires coordinated effort of a team of scientists. Once the community achieves consensus on CCSNe dynamics and outcomes from these new-generation simulations, it will be natural to refresh the parameterized models and update the predictions of observable quantities.

The rate of data accumulation on CCSNe and astronomical transients has been increasing thanks to new surveys. This trend will continue in the future, but already now it is not possible to obtain sufficient followup data for most of the discovered events. The followup of the discoveries is typically prioritized based on the perceived astrophysical interest, which creates a need for theoretical exploration of often extreme physical situations.

Based on these trends, I plan to focus my efforts on theoretical explanation of rare and unique events. Specifically, I plan to exploit synergy between my past work on theory and data modeling of CCSNe with my ongoing work on binary star interactions (Chapter 2). For example, I would like to explore the connection between CCSN environment and binary evolution, strengthen the connection between stellar mergers and peculiar CCSN explosions like SN1987A, and apply the new tools we are developing for binary interactions.

Chapter 2

Death of binary stars

2.1 Overview

Stars are often members of binary or multiple systems. About half of solar-type stars have companions and the fraction rises considerably for more massive stars (e.g. Raghavan et al., 2010; Moe and Di Stefano, 2017). A significant fraction of the binaries exchange mass at some point of their evolution. Typically, mass transfer commences when one of the stars expands as a consequence of stellar evolution. Alternatively, the orbit can shrink as a result of loss of angular momentum from the binary, for example due to magnetized stellar wind or tidal dissipation. The gas infalling on the companion often carries significant angular momentum, which can lead to formation of an accretion disk. The accretion on the companion releases gravitational potential energy, which can significantly affect the observed emission from the binary, especially if the companion is a compact star such as WD, NS, or BH. There are a myriad of astrophysical phenomena associated with mass transfer in binary stars, which we cannot fully review here.

Another ingredient in binary star evolution is the rapid phase of *common envelope evolution* (CEE). CEE is relatively frequent compared to events like SN explosions. Based on binary population models and observed transient events, Kochanek et al. (2014) estimated the CEE rate in our Galaxy between 0.2 and $0.5\,\mathrm{yr}^{-1}$. The event rate is dominated by low-mass binaries, but CEE is very important for shaping the population of massive stars. Sana et al. (2012) analyzed the population of Galactic massive binaries and found that only about 30% of the systems are sufficiently separated to effectively evolve as two single stars. Out of the rest, about 25% will merge, 14% might enter and survive CEE as binaries, and the rest experiences some kind of mass transfer.

CEE can significantly reduce the binary semi-major axis and therefore plays a crucial role in evolutionary scenarios leading to close binaries composed of at least one compact object (WD, NS, BH). This includes cataclysmic variables, X-ray binaries, and recycled pulsars. Objects of special interest are close double compact object binaries, which efficiently lose orbital angular momentum due to gravitational wave emission to merge within the age of the Universe. Gravitational waves accompanying BH and NS mergers have recently been detected with gravitational-wave interferometers LIGO and Virgo, which has spurred renewed interest in CEE. An alternative outcome of CEE is a merger of the binary components into a single object. In such cases, the remnants should appear as rapidly spinning and possibly magnetic stars, which potentially includes blue stragglers or mysterious objects such as the progenitors of SN1987A, SN2009ip, η Car, and long

γ-ray bursts (e.g. Paczynski, 1976; Iben and Livio, 1993; Fryer and Heger, 2005; Morris and Podsiadlowski, 2007; Mauerhan et al., 2013a; Portegies Zwart and van den Heuvel, 2016; Schneider et al., 2016; Hirai et al., 2021).

CEE is a very important and largely unsolved problem of binary star evolution, which has attracted significant attention from theorists and observers. Developing analytical and numerical theory of CEE is difficult, because it requires resolving a vast range of temporal and spatial scales often ranging from a NS ($\sim 10\,\mathrm{km}$) to a red supergiant ($\gtrsim 10^8\,\mathrm{km}$). Observational constraints on CEE have so far mostly relied on comparing stellar populations before and after CEE, but recent detections of associated transient brightenings have opened new ways of studying these events. In the following description of CEE, I will focus predominantly on the aspects that are relevant to my work covered in subsequent sections. CEE is thoroughly reviewed in dedicated works (e.g. Iben and Livio, 1993; Taam and Sandquist, 2000; Ivanova et al., 2013b).

2.1.1 Stages of common envelope evolution

CEE can occur as an outcome of mass transfer in binary stars. Stability of the mass transfer depends on the response of the star to mass loss in relation to the changes of the orbital properties that accompany the redistribution of mass and angular momentum within the binary. In most cases, the mass transfer proceeds on the nuclear or thermal timescale of the mass-losing star. In some cases, however, the mass transfer cannot be stabilized and runs away on a timescale that approaches the dynamical timescale of the binary (essentially its orbital period) and the binary enters the CEE.

Dynamically-unstable mass transfer is not the only way to initiate CEE in a binary star. The tidal Darwin instability occurs when the orbital angular momentum is insufficient to maintain synchronous spin of one or more of the binary components (e.g. Eggleton and Kiseleva-Eggleton, 2001). Typically, this happens when the more massive primary star expands due to its nuclear evolution and its moment of inertia increases. Tides try to synchronize the spin by transferring angular momentum from the orbit to the primary star, which leads to orbital decay. If the orbital angular momentum is too small, the orbit does not stabilize and the binary spirals in on the tidal timescale. Typically, the threshold for Darwin instability is formulated in the terms of critical mass ratio q_{crit} of the binary components. For contact binary stars, which are stars on such a small orbit that they share a tenuous envelope, $q_{\mathrm{crit}} \approx 0.1$ (Rasio, 1995; Rucinski, 2001). Another possibility to enter the CEE is a collision, where the two stars approach each other on a hyperbolic or extremely elliptic orbit. Such a situation could arise due to various effects in the dynamics of three or more bodies. One example are stellar collisions due to the Lidov–Kozai effect (e.g. Thompson, 2011; Katz and Dong, 2012; Pejcha et al., 2013; Naoz and Fabrycky, 2014).

The first stage of CEE is a gradual loss of corotation of the stellar spins and the orbit, which accompanies the accelerating mass transfer in the binary. This phase is not applicable to stellar collisions. Loss of corotation is difficult to model with 1D stellar evolution codes, because of extreme binary properties like mass transfer rate and because the approximation of spherical symmetry becomes invalid. For 3D explicit hydrodynamics, the involved timescale is too long. In my research, I have argued that processes happening during this under-appreciated phase are important for the final outcome of CEE and especially for the brightenings that accompany them. I give more details in Section 2.1.2.

When the evolution of the binary proceeds sufficiently fast, it is advantageous to think about the system not in terms of the Roche potential, but rather as if the secondary star spirals inside a non-corotating envelope (Paczynski, 1976; Meyer and Meyer-Hofmeister, 1979). The envelope exerts hydrodynamic drag on the secondary star, which leads to dissipation of the orbital energy (e.g. Fryxell and Taam, 1988; MacLeod and Ramirez-Ruiz, 2015). The envelope becomes partially or completely unbound. Computer simulations have often not been able to simulate the expected envelope ejection, although some of the recent more realistic simulations report higher unbound fractions of the envelope (e.g. Nandez et al., 2015; Ohlmann et al., 2016; Reichardt et al., 2020; Sand et al., 2020). Even partial envelope ejection is accompanied by a luminous transient, which we describe in more detail in Section 2.1.3. It is also possible that the envelope expansion and the associated decrease of density slows down the inspiral, which enters into a long-lasting self-regulated phase, possibly followed by another dynamical instability. Other physical processes like jets, pulsations, or dust-driven winds might help envelope ejection (e.g. Papish et al., 2015; Shiber et al., 2019; Schreier et al., 2019; Clayton et al., 2017; Glanz and Perets, 2018). In the end, the envelope is either completely ejected and the binary survives or only part of the envelope becomes unbound and the two stars merge. When the binary survives, the semi-major axis is significantly reduced. If the two stars merge, the remnant evolves on the thermal timescale toward thermal equilibrium and the signatures of the violent interaction gradually disappear (e.g. Sills et al., 1997, 2001; Glebbeek et al., 2009).

Traditionally, CEE is assumed to be a dynamic event, which can be interpreted using energy conservation. The outcome of CEE is usually predicted by equating the binding energy of the envelope to the difference between initial and final orbital energies, which gives the final orbital separation. A free parameter, common envelope efficiency α, is introduced to quantify the fraction of orbital energy available for unbinding of the envelope (e.g. Webbink, 1984; Livio and Soker, 1988). Many aspects of this energy formalism have been thoroughly scrutinized and contentious points have been identified. For example, it is unclear how to calculate the envelope binding energy, which form of energy is actually available for unbinding of the envelope, how important are certain features of the realistic equation of state such as the recombination of ions, or whether radiative losses are important (e.g. Xu and Li, 2010; Ivanova and Chaichenets, 2011; Ivanova et al., 2015; Grichener et al., 2018). Inferences of α from observed populations imply $\alpha \gtrsim 1$ for certain classes of objects, which might indicate that CEE extends to the thermal timescale and that angular momentum conservation is more appropriate description of CEE (e.g. Nelemans et al., 2000, but see Webbink, 2008). Nonetheless, CEE energy formalism is often used in rapid binary population synthesis to predict numbers of various close binary systems and rates of cataclysmic events due to such binaries (e.g. Belczynski et al., 2002; Dominik et al., 2012).

In the subsequent Sections, I describe my contribution to several contemporary aspects of CEE. Section 2.1.2 explores mass loss from the binary preceding the main dynamical event. This phenomenon turns out to be important for understanding the observed transient brightenings that accompany CEE, which I discuss in Section 2.1.3. Section 2.1.4 describes work on planetary nebula Sh 2-71, where the envelope ejection from a binary star was influenced by a nearby tertiary star. Finally, Section 2.1.5 describes our first steps in understanding populations of binary stars in modern photometric and spectroscopic time-domain surveys.

2.1.2 Hydrodynamics of L2 outflows

Mass transfer is binary stars in usefully described by motions inside a Roche potential. In this approximation, stars are modeled as point masses on a circular orbit and the reference frame is set to corotate with the orbit. As a result, the Roche potential is a combination of point-mass potentials from both stars and a potential arising from the centrifugal force. Equations of motion include also the Coriolis force. There are 5 Lagrange points in the Roche potential. L1, L2, and L3 are saddle points of the Roche potential located on the line connecting both stars so that L1 lies between them, L2 on the side of the lower-mass component, and L3 on the side of the higher-mass component. L4 and L5 are located off the binary axis and are of less importance for the processes in binary stars.

Mass transfer starts when one of the stars fills its Roche lobe by expanding its photosphere to or beyond the L1 point. Mass flows from the donor star through L1 point to the accretor. If the mass-transfer rate is too high, the accretor cannot efficiently absorb the incoming material and expands. Ultimately, the gas starts to leak out from the binary near the L2, although the exact nature of this process is unclear especially when the mass-transfer rate is very high (e.g. Sytov et al., 2007). Alternatively, a contact binary can shrink its orbit, for example due to the Darwin instability, so that the envelope shared by the two components overflows L2 (e.g. Webbink, 1976). In some stars, the pressure scale height of their atmospheres becomes comparable to the physical distance between equipotentials passing through L2 and L3. As a result, L2 overflow will be accompanied by additional loss of mass from L3.

The dynamics of gas leaving L2 was first studied by Kuiper (1941). A more systematic understanding was provided by Shu et al. (1979), who analyzed the properties of cold streams launched from L2 and in corotation with the orbit. The stream center follows the ballistic trajectory of a test particle while the stream spreading is determined by the internal energy and tides due to the central binary. A test particle at corotation at L2 is always bound with negative total energy, but as it leaves the binary it gains energy and angular momentum due to tidal torques from the time-changing gravitational field of the central binary. Shu et al. (1979) found that streams leaving binaries with mass ratios $0.064 \leq q \leq 0.78$ become unbound and form an equatorially-concentrated spiral outflow. For the remaining q, tidal torquing is inefficient and the stream returns, likely forming a viscous circumbinary disk.

In Hubová and Pejcha (2019), which is shown in full in Section 3.2.1, we investigated trajectories of test particles leaving binary stars from the vicinity of L2. We improved on Shu et al. (1979) by injecting the particles not exactly at L2 but at a range of nearby positions and by giving the particles non-zero initial velocities in the corotating frame. We identified two new types of ballistic trajectories, which either collide with the binary surface or loop and self-intersect close to the binary forming a hydrodynamic shock. We mapped the non-trivial distribution of outcomes as a function of initial position and velocity and we found that even particles launched sub-synchronously with respect to the binary orbit can under some circumstances achieve positive total energy. This finding is important for the interpretation of some observations, which point to radiatively-inefficient unbound outflows from sub-synchronously spinning binary stars (Sec. 2.1.3).

Although ballistic trajectories in the Roche potential serve as an important tool for understanding the dynamics of the outflow, interpretation of observations requires a more sophisticated approach. In Pejcha et al. (2016a), which is shown in full in Section 3.2.2,

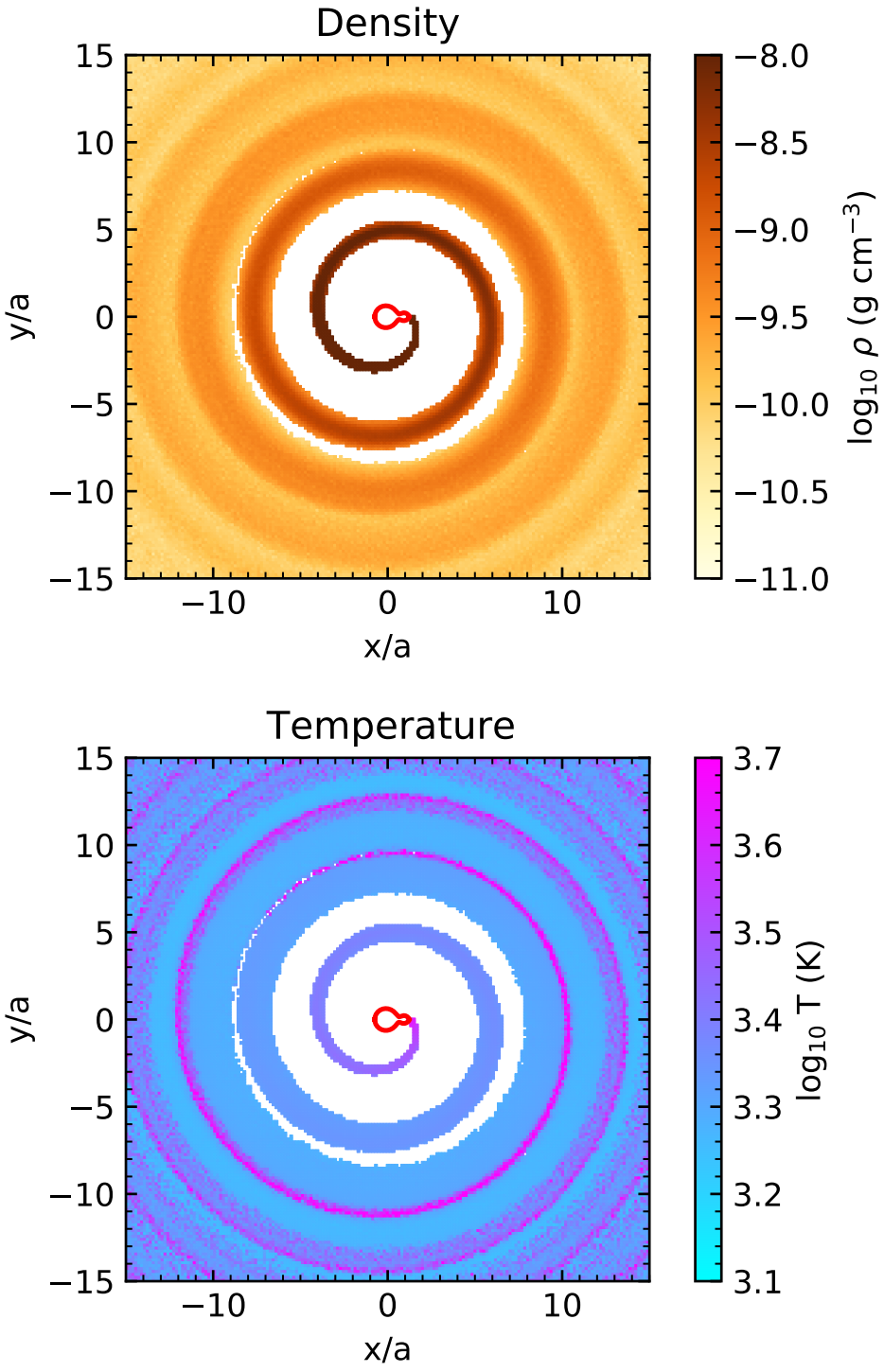

Figure 2.1: Density (top) and temperature (bottom) structure of outflow launched from the L2 point in corotation with the binary orbit. The results were obtained with a SPH code with realistic equation of state and including artificial viscosity. Radiative processes (diffusion, cooling, irradiation) were not included. Red closed line in both panels shows the critical equipotential of the Roche model, which passes through the L2 point. The binary parameters are similar to the models of V1309 Sco (Pejcha et al., 2017).

we have developed a new smoothed-particle hydrodynamics (SPH) code specially suited for investigating outflows from binary stars. Unlike many other CEE simulations based on SPH, which focus on resolving the hydrodynamics and self-gravitational interactions inside the common envelope, our approach describes the two stars as point masses and instead realistically simulates the outflow. We inject SPH particles near the L2 point and follow their evolution taking into account shocks, which are in SPH traditionally resolved with artificial viscosity, radiative diffusion, radiative cooling perpendicular to the orbital plane, and irradiation from the central binary. These processes are implemented using realistic equation of state, which includes hydrogen and helium ionization as well as molecular hydrogen, and opacity tables with several options for the properties of dust.

Our results in Pejcha et al. (2016a) verify the basic findings of Shu et al. (1979): the division between bound and unbound outflows is controlled by the binary mass ratio. Surprisingly, we discovered that even unbound outflows experience internal shocks, which arise as the expanding spiral stream expands in the orbital plane and collides with itself. An example of this effect is visible as a spiral in Figure 2.1. The horizontal expansion is caused partially by the gas pressure and partially by the differential tidal torques from the central binary. The shocks thermalize non-negligible fraction of the kinetic energy of the outflow, which leaks out of the disk vertically as radiation. Our estimated radiative luminosities and temperatures roughly match the range seen in the candidate optical counterparts of CEE (Sec. 2.1.3). However, very high mass-loss rates necessary to match the observed luminosities require a long time to build up the outflow and to have the light diffuse out of it. Instead, radiative L2 outflows powered by internal shocks are very promising explanation of pre-maximum luminosity increase seen in many candidate optical counterparts as will be explained in Section 2.1.3.

In Pejcha et al. (2016b), which is shown in full in Section 3.2.3, we continued our investigation of radiation hydrodynamics of L2 outflows and explored in more detail the bound outflows. Here, we found that the efficiency of radiative cooling dramatically affects the outflow configuration. For efficient radiative cooling, which can be parameterized by the ratio of diffusion to advection timescales, the bound outflow returns and forms a viscously-evolving disk-like structure, as originally envisioned by Shu et al. (1979). For inefficient radiative cooling, the material piles around the binary and continues to receive mass and energy. This leads to an almost isotropic wind-like outflow. For the small part of parameter space where the energy injection and radiative cooling are almost in balance, we found an inflated envelope that transports, reprocesses, and radiates energy input from the vicinity of the binary. In all cases, the radiative efficiency is quite high, although the details quite likely depend on the treatment of viscosity in the SPH method. So far, circumbinary bound disks have not been clearly identified in pre-explosion data of CEE transients.

2.1.3 What powers luminous red novae?

Some of the first transient brightenings that we now associate with CEE were M31 RV discovered in 1988 (Mould et al., 1990) and V4332 Sgr, which erupted in 1994 (Martini et al., 1999). Initially, these objects were interpreted as peculiar novae, which showed unusual low-temperature spectra and did not exhibit the evolution to high ionization commonly seen in classical novae. Interest in these transients has dramatically increased after the discovery of V838 Mon in 2002 (e.g. Brown et al., 2002; Munari et al., 2002;

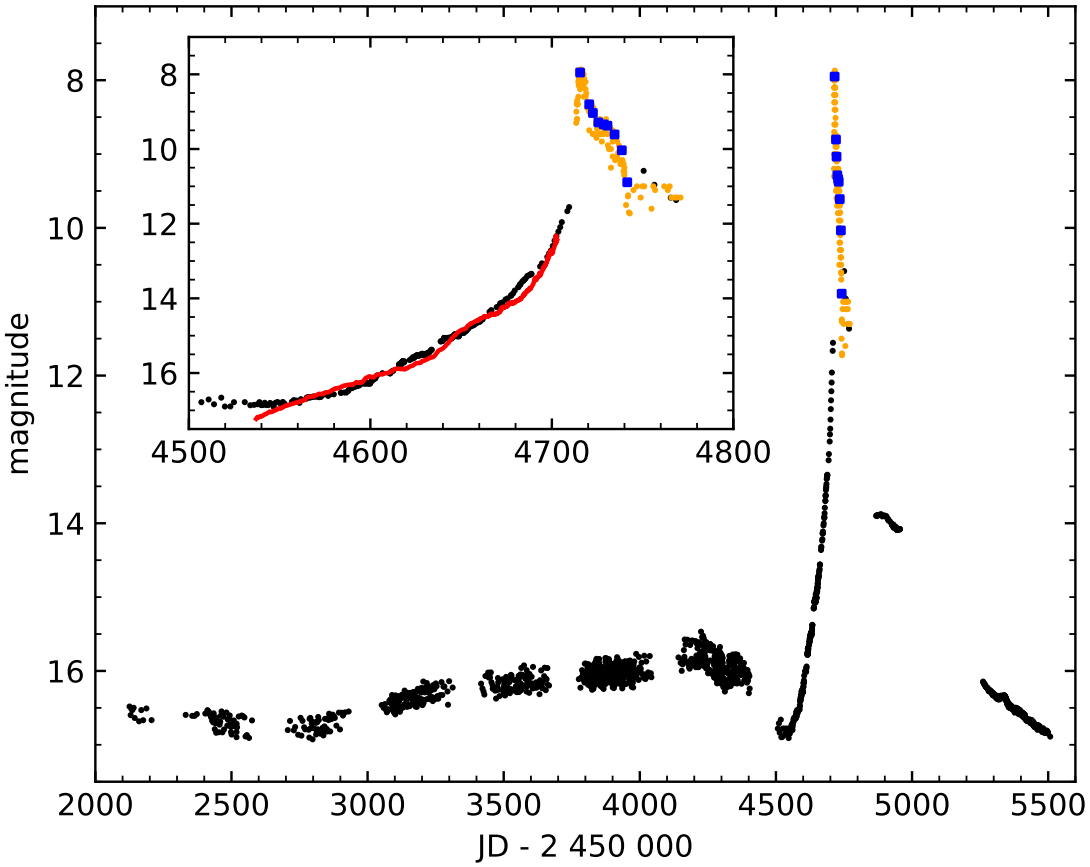

Figure 2.2: Light curve of V1309 Sco. Black points shows I-band observations from OGLE (Tylenda et al., 2011), orange points visual magnitudes from AAVSO, and blue squares V-band measurements from ASAS. The inset plot shows the detail of the rise to the maximum with one of our SPH simulations overplotted with a red line. More details are given in Pejcha et al. (2017).

Sobotka et al., 2002). Its high luminosity exceeding $10^5\,L_\odot$, low effective temperature plummeting to about 2000 K, and spectacular light echoes captured by the Hubble Space Telescope spurred theoretical interest. Out of many theories, strong interactions between stars have been able to explain most of the observations of V838 Mon as well as previous events (e.g. Soker and Tylenda, 2003; Tylenda and Soker, 2006).

A breakthrough event was V1309 Sco, which exploded in 2008 (Mason et al., 2010). Its pre-outburst observations were recorded by the OGLE project and analyzed by Tylenda et al. (2011). These observations, shown in Figure 2.2, revealed that V1309 Sco was a contact binary with rapidly decreasing orbital period accompanied by a gradual change of the phased light curve. In early 2008, V1309 Sco started its brightening, which culminated in an outburst about 200 days later. These observations provide unequivocal proof that V1309 Sco was caused by a binary star interaction.

Another important insight into these transients was provided by Ivanova et al. (2013a), who noticed similarity between the light curves of events similar to V1309 Sco and Type IIP SNe. Ivanova et al. (2013a) used analytic scaling relations of Type IIP SNe, which we explain in Section 1.1.3, to argue that CEE transients are powered by diffusion of light through an expanding and recombining hydrogen shell. This idea was further quantitatively explored by Lipunov et al. (2017) and MacLeod et al. (2017) among others.

We now know approximately 20 events similar to V1309 Sco or V838 Mon, which are often called Luminous Red Novae (LRNe), Intermediate Luminosity Optical Transients (ILOTs), mergerbursts, and other variations of these terms (e.g. Kashi and Soker, 2010; Pastorello et al., 2019; Blagorodnova et al., 2021). Many of them show complicated light curves with two peaks, gradual pre-explosion brightenings, and dust formation. However, the interpretation of many events with luminosities similar to LRNe and ILOTs is not straightforward. There is evidence that some of these objects are luminous blue variable outbursts or faint electron-capture SNe rather than stellar mergers (e.g. Pastorello and Fraser, 2019). Developing precise criteria for observational identification of optical counterparts of CEE is needed.

My initial ideas about LRNe were published as Pejcha (2014), which is shown in full in Section 3.2.4. In this work, I analyzed three features of the pre-maximum light curve of V1309 Sco: (i) the directly observed orbital period change accelerated on a timescale $P/\dot{P} \approx \dot{P}/\ddot{P} \approx 2\,\mathrm{years}$, which is much shorter than the tidal or thermal timescale of the binary (hundreds to thousands of years) and much longer than its dynamical timescale (roughly the orbital period $P \approx 1.4\,\mathrm{days}$), (ii) the gradually changing shape of the phased light curve occurred with a similar slow pace as the orbital period change, while the total observed period change of 2–3% suggests that the physical dimensions of the system changed only by a small amount, and (iii) the slow gradual rise to the peak appears to be an extension of the previous trends and cannot be easily explained by a simple instantaneous mass ejection. I proposed that this observed sequence of events can be explained V1309 Sco experiencing mass loss from the L2 point with gradually increasing mass-loss rate and that the mass-loss rate history can be, in principle, reconstructed from the observations.

In Pejcha et al. (2017), which is shown in full in Section 3.2.5, we verified the ideas presented in Pejcha (2014) using the SPH code developed in Pejcha et al. (2016a,b). First, we set up an analytic model of the L2 spiral stream and calibrated its properties based on SPH simulations relevant for V1309 Sco. Then, we raytraced through the model to calculate phased light curves. By gradually increasing the mass-loss rate we naturally

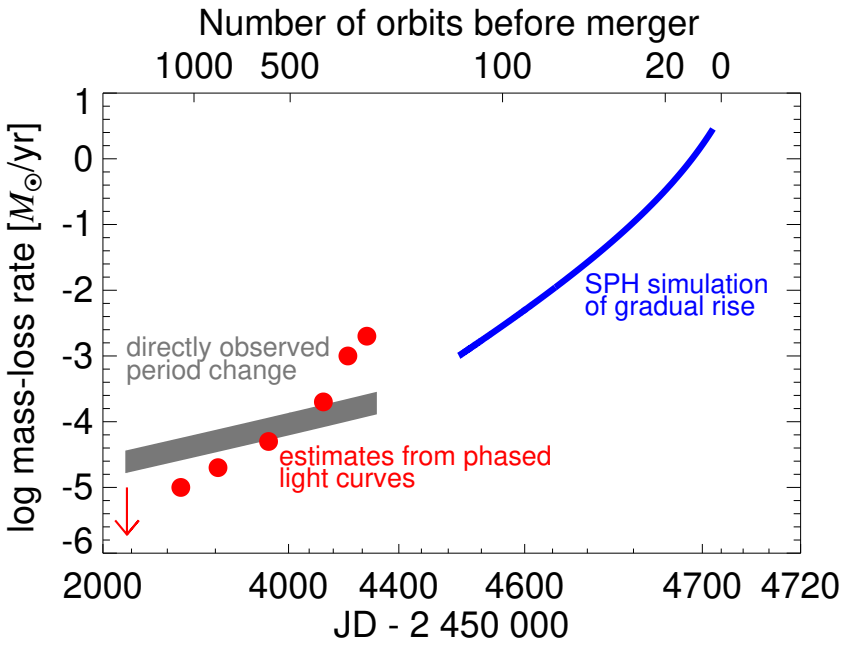

Figure 2.3: Mass loss history of V1309 Sco. Red points show mass-loss rates estimated from the seasonal phased light curves, gray bar shows the inference from directly observed orbital period change assuming L2 mass loss and binary mass ratio compatible with the the observed phased light curve, and the blue line marks the prescribed mass-loss rate evolution that explains the gradual rise to the maximum shown in the inset panel of Fig. 2.2. This figure is based on Pejcha et al. (2017), except that here I fixed the error affecting the inferences from the period change.

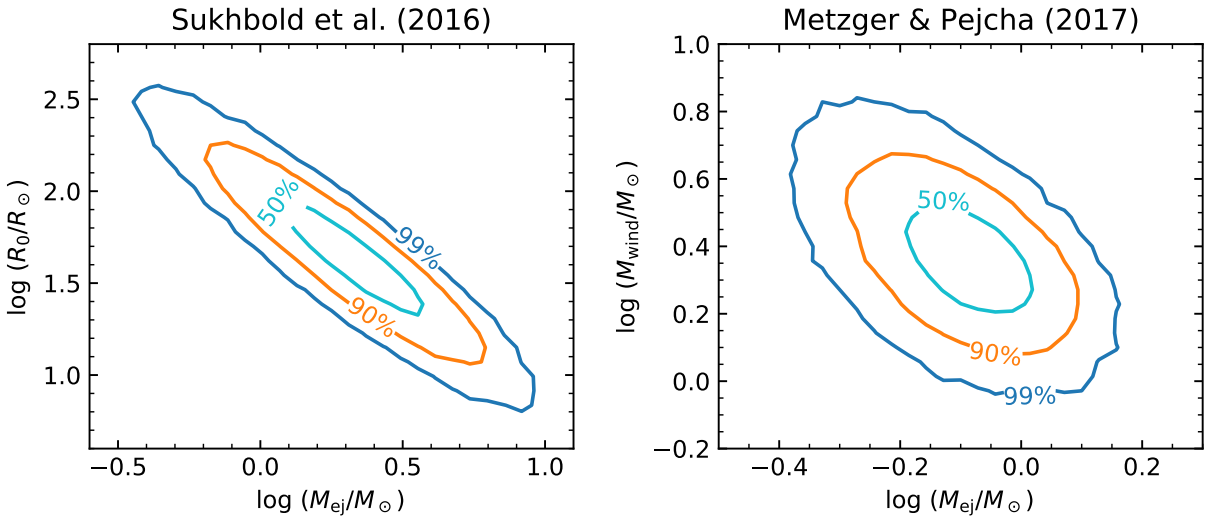

Figure 2.4: Explosion properties of luminous red nova AT 2018bwo. Left panel shows the inferences of ejecta mass $M_{\rm ej}$ and initial radius R_0 based on Type II-P SN scaling relations. Right panel shows the mass of the dynamical ejecta $M_{\rm ej}$ and the mass in the pre-existing equatorially-focused wind $M_{\rm wind}$ based on scaling relations of shock-powered transients of Metzger and Pejcha (2017). Quantitative results from this analysis are described in Blagorodnova et al. (2021).

reproduced the sequential change from double-peaked to single-peaked phased light curve. By comparing the theoretical and observed light curves, we estimated the mass-loss history and found that it approximately explains the directly observed change of the orbital period. These findings are illustrated in Figure 2.3. Central binary can only be obscured by the L2 spiral stream for a certain range of orbital inclinations, which help us to break the degeneracy between the observed amplitude, inclination, and mass ratio of the binary. Based on these ideas, we constrained the binary mass ratio to $0.07 \lesssim q \lesssim 0.10$. This value is similar to $q_{\rm crit}$ for the Darwin instability, which suggests that the inspiral might have been initiated by the tidal Darwin instability. Nonetheless, the high value of $\dot{P}$ and $\ddot{P}$ as well as quantitative agreement with angular momentum loss from L2 suggest that L2 mass loss was the dominant driver of period change in the few years before the main peak.

In Pejcha et al. (2017), we also performed SPH simulation of the final approximately 200 days before the main peak, when the binary was already enshrouded in the L2 outflow. This time period corresponds to approximately 150 original orbital periods, which can be directly simulated by our SPH code that neglects the internal dynamics inside the binary star. We prescribed a runaway increase of the L2 mass-loss rate and we self-consistently evolved the binary orbital properties including the injection point of the particles in response to the loss of angular momentum from the binary. We could reproduce the observed gradual rise, as we show in the inset panel of Figure 2.2, and reconstruct the mass-loss history of V1309 Sco up to several days before the main peak, as we illustrate in Figure 2.3. By integrating the mass-loss history, we estimated that V1309 Sco lost about $0.05\,M_\odot$ through L2 before the evolution of the binary became dynamical. To summarize, in Pejcha et al. (2017), we quantitatively explained the pre-maximum observations of V1309 Sco with a unified model of runaway L2 mass loss.

The pre-dynamical mass loss is followed by a dynamical mass ejection, which likely occurs more isotropically and with faster velocity. Specifically, Ivanova et al. (2013a) and Nandez et al. (2014) performed CEE simulations of V1309 Sco and predicted the mass in the dynamical ejection to lie between 0.04 and $0.09\,M_\odot$. This number is comparable with the total pre-dynamical mass loss estimate of Pejcha et al. (2017). As a result, it is likely that the two different ejecta components moving with different velocities will collide and that the observed plateau-like light curve might not be explained simply as light diffusing out of an expanding and recombining hydrogen shell.

We explored the observational consequences of shock interaction in LRN ejecta in Metzger and Pejcha (2017), which is shown in full in Section 3.2.6. In this work, we constructed a semi-analytic model of shock interaction between a pre-existing equatorially-focused wind and a faster spherical ejecta, which includes emission of radiation and transfer of radiation from the shock to the spherical component. We argued that the first peak seen in the light curves of LRNe is caused by cooling of shock-heated ejecta expanding in the polar direction, while the second peak is due to the diffusion of light from the radiative shock through the ejecta. In some cases, the spherical component can engulf the equatorial shock and we would see a light curve with a bright shock-powered plateau, similarly to some SNe (Sec. 1.1.4). The dense shock-cooled region is also an ideal site for dust formation, which is often seen in late observations of LRNe and their remnants. For giant progenitors, the dust forms when the shock luminosity is still high, which can lead to long infrared-bright transients, perhaps similar to events recently identified with the Spitzer Space Telescope (Kasliwal et al., 2017).

In Metzger and Pejcha (2017), we provided also simple analytic and observationally-testable relations to estimate luminosities and durations of LRN light curves. One of the first applications of these relations to the observed data was done by Blagorodnova et al. (2021) and we illustrate the results in Figure 2.4. This work is a first step in solving one of the current open problems of LRNe: are their light curves powered simply by diffusion of light out of a recombining hydrogen shell or does shock heating play a dominant role? This is not an easy question to answer, because the observational appearance might be very similar in both cases. The path forward is to carefully compare inferences of the ejecta masses from the two models and contrast them with other properties of the transient. For example, if the mass of the recombining hydrogen shell required to explain the light curve exceeds the progenitor mass, then the ongoing shock interaction is the preferred explanation.

2.1.4 Irregular shapes of planetary nebulae

A single low-mass star should end its live by ejecting a nearly spherical planetary nebula. Yet, many planetary nebulae show axisymmetric structures, which are best explained by the binarity of the central object and ejection of the CEE (e.g. De Marco, 2009; Jones and Boffin, 2017). We also know that many low-mass stars are members of triples or higher-order multiples and that this should play a role in the formation of some planetary nebulae. Triple-star interactions have also been recently considered in the CEE hydrodynamics (Glanz and Perets, 2021). Despite the observed triple statistics, we know only very few irregular irregular planetary nebulae that require interactions in a triple system (e.g. Bear and Soker, 2017).

In Jones et al. (2019), which is shown in full in Section 3.2.7, we argued that Sh 2-71 is one of the best candidates for planetary nebulae shaped by triple star interactions. Sh 2-71 is known to have an irregular shape and there are two candidate central objects. The brighter one is a peculiar variable central star with an unusual light curve and a period of about 68 days, which is likely associated with motions in an unresolved binary star. However, this object is offset from the apparent center of the nebula and is also too cold to provide enough ionizing photons (Mikulášek et al., 2007; Močnik et al., 2015). Little is known about the second star, which is much fainter but also likely hotter and closer to the nebula center. In Jones et al. (2019), we presented a discovery of two new distant emission regions of Sh 2-71, which are approximately aligned with the two candidate central objects. We also argued that the system was originally a triple star system, where the most massive star was the single outer component. Lidov–Kozai cycles in the triple system could have decreased the orbital period of the binary subsystem. When the more massive star ejected the planetary nebula, the sudden loss of mass caused the triple system to break up. Some of the planetary nebula mass could have been captured in the binary star system, which might be responsible for the peculiar variability or the distant emission regions. We supported this scenario with numerical integrations of binary orbits responding to mass loss taking into account the mass ejection timescale, Lidov–Kozai timescale, and the main-sequence lifetime of the more massive component. The inferred mutual velocities are compatible with current best relative proper motion estimates from Gaia.

2.1.5 Effects of binary evolution of stellar populations

Traditionally, observational constraints on the physics of CEE have been obtained by comparing populations of progenitor binaries with post-CEE systems with the aim to constrain the CEE energy formalism (e.g. Nelemans et al., 2000; Zorotovic et al., 2010; De Marco et al., 2011). Similar investigations can become more powerful with the current and upcoming time-domain photometric and spectroscopic surveys, which greatly expand the amount and quality of available data.

In Pawlak et al. (2019), which is shown in full in Section 3.2.8, we analyzed photometric variability of stars observed by the time-domain spectroscopic survey APOGEE. As a part of the Sloan Digital Sky Survey, APOGEE obtains high-resolution high S/N spectra of stars in the near infrared, often at multiple epochs for each target (York et al., 2000; Majewski et al., 2017). The primary motivation of our work was to identify eclipsing binaries in the overlap of APOGEE and ASAS-SN, because the number of APOGEE epochs is typically insufficient to fully characterize the binary orbit with spectroscopic data alone and because absolute orbital properties cannot be determined only from photometry. We searched for photometric variability in more than 250,000 APOGEE targets with V-band data from the All-Sky Automated Survey for Supernovae (Shappee et al., 2014; Kochanek et al., 2017). Typical stars had over 150 photometric measurements distributed over few years. We identified almost 2000 variable stars of which more than 400 were new discoveries. Among these stars, we found over 400 eclipsing binaries and ellipsoidal variables, more than 100 classical pulsating stars, and more than 700 long-period pulsating red giants. By our independent method, we found that binary stars are found preferentially at lower metallicity, which agrees with findings by other groups (Badenes et al., 2018; Moe et al., 2019). One of our eclipsing binaries was recently investigated in more detail by Miller et al. (2021). We also explored characterization of the variability using non-periodic Gaussian damped random walks.

2.2 Additional co-authored works

- **Jayasinghe et al. (2019a,b, 2020a,b,c, 2021a)**

  This series of papers characterizes time-variability of stars in ASAS-SN. Jayasinghe et al. (2019a) updated classifications of known variables stars, Jayasinghe et al. (2019b) found new variable stars in one of the fields continuously observed by the TESS satellite, Jayasinghe et al. (2020a) characterized stellar variability in the southern sky, Jayasinghe et al. (2020c) studied pulsating variables of δ Sct type, Jayasinghe et al. (2020b) discovered heterogeneity of contact binaries related to the structure of surface convection zones, and Jayasinghe et al. (2021a) combined photometric variability with information from spectroscopic surveys for variable stars across the whole sky. Our work covered in Section 3.2.8 (Pawlak et al., 2019) is a part of this series of papers.

- **Aydi et al. (2020)**

  This paper presents simultaneous observations of a classical nova V906 Car in γ-rays from the Fermi satellite and in the optical from the BRITE nanosatellite. Small flares are seen simultaneously in both bands, which points to an underlying shock interaction that powers the outburst.

- **Williams et al. (2020)**

  This work presents photometry and spectroscopy of ILOT AT 2019abn, which could have been caused by a stellar merger.

- **Blagorodnova et al. (2021)**

  This submitted paper studies LRN AT 2018bwo in NGC 45 and its yellow supergiant progenitor. For the first time, progenitor and transient observations are combined with tailored binary evolution models and theoretical interpretation of the outburst light curve. An illustration of the theoretical modeling of the transient is shown in Figure 2.4.

2.3 Future work

My future work will be focused along three main lines. First, I plan to significantly develop theoretical methods that are used to study CEE. With the members of my group, we are working on coupling a special version of moving-mesh hydrodynamics with radiative transport in the flux-limited diffusion approximation. Once finished, this code will allow us to study multi-dimensional behavior of LRNe over many orders of magnitude of spatial and temporal scales. We will be able to predict observational appearance and study even more complex phenomena related to the formation of dust and molecules. This code is also much more widely applicable to all astronomical transients, where multi-dimensional effects are important. I also plan to address the gap between 1D stellar evolution codes, which are used to study CEE long before or after the dynamical phase and explicit multi-dimensional hydrodynamic codes, which simulate the short dynamical phase. This could be achieved with low-Mach number hydrodynamics, which evolves perturbations on slowly-changing hydrostatic background and which does not have restrictions on the timestep due to the sound speed. This would be an ideal tool to study internal structure of binaries in the long pre-dynamical phase of CEE or the evolution of angular momentum on intermediate timescale after a merger. I will opportunistically complement these investigations with analytic and semi-analytic models addressing topics such as stability of mass transfer in binary stars, generation of magnetic fields in CEE, or loss of angular momentum by outflows from binary stars.

Second, with the new tools available I plan to make new predictions, compare them with observations, and provide new constraints on the CEE theory. I will address open questions such as: are all LRNe are all caused by slowly inspiralling binaries or do some of them come from binary collisions? Are all optical LRNe stellar mergers? Are the recently-identified long and cool infrared transients bona fide CEE events that leave behind surviving binaries? Are LRNe powered simply by diffusion or by shock interaction? How do ejecta masses and energies of LRNe compare to CEE predictions and what does this imply for astrophysically-important stellar populations? What happens inside binary stars as they approach CEE? How are magnetic fields amplified? What happens after the merger in terms of angular momentum redistribution and magnetic field evolution? Can we make correspondence to NS mergers? What will be the observational appearance of merger remnants and can we identify them in astronomical surveys?

Finally, I plan to utilize the current and upcoming photometric and spectroscopic time-domain surveys to constrain CEE theory and binary and multiple star interactions

in general. For example, with my group we are working on constraining the properties of tidal Darwin instability in populations of contact binaries and on explaining the observed gap in the distribution of effective temperatures of contact binaries. Other topics that interest me are long-term changes and spot evolution in binary stars, identification and analysis of peculiar objects, and hunt for remnants of stellar mergers.

Bibliography

Adams, S. M., C. S. Kochanek, J. F. Beacom, M. R. Vagins, and K. Z. Stanek: 2013, 'Observing the Next Galactic Supernova'. *Astrophys. J.* **778**(2), 164.

Anderson, J. P., S. González-Gaitán, M. Hamuy, C. P. Gutiérrez, M. D. Stritzinger, F. Olivares E., M. M. Phillips, S. Schulze, R. Antezana, L. Bolt, A. Campillay, S. Castellón, C. Contreras, T. de Jaeger, G. Folatelli, F. Förster, W. L. Freedman, L. González, E. Hsiao, W. Krzemiński, K. Krisciunas, J. Maza, P. McCarthy, N. I. Morrell, S. E. Persson, M. Roth, F. Salgado, N. B. Suntzeff, and J. Thomas-Osip: 2014, 'Characterizing the V-band Light-curves of Hydrogen-rich Type II Supernovae'. *Astrophys. J.* **786**(1), 67.

Andrews, J. E. and N. Smith: 2018, 'Strong late-time circumstellar interaction in the peculiar supernova iPTF14hls'. *MNRAS* **477**(1), 74–79.

Arcavi, I.: 2017, 'Hydrogen-Rich Core-Collapse Supernovae'. In: A. W. Alsabti and P. Murdin (eds.): *Handbook of Supernovae*. Springer International Publishing, p. 239.

Aydi, E., K. V. Sokolovsky, L. Chomiuk, E. Steinberg, K. L. Li, I. Vurm, B. D. Metzger, J. Strader, K. Mukai, O. Pejcha, K. J. Shen, G. A. Wade, R. Kuschnig, A. F. J. Moffat, H. Pablo, A. Pigulski, A. Popowicz, W. Weiss, K. Zwintz, L. Izzo, K. R. Pollard, G. Handler, S. D. Ryder, M. D. Filipović, R. Z. E. Alsaberi, P. Manojlović, R. Lopes de Oliveira, F. M. Walter, P. J. Vallely, D. A. H. Buckley, M. J. I. Brown, E. J. Harvey, A. Kawash, A. Kniazev, C. S. Kochanek, J. Linford, J. Mikolajewska, P. Molaro, M. Orio, K. L. Page, B. J. Shappee, and J. L. Sokoloski: 2020, 'Direct evidence for shock-powered optical emission in a nova'. *Nature Astronomy* **4**, 776–780.

Badenes, C., C. Mazzola, T. A. Thompson, K. Covey, P. E. Freeman, M. G. Walker, M. Moe, N. Troup, D. Nidever, C. Allende Prieto, B. Andrews, R. H. Barbá, T. C. Beers, J. Bovy, J. K. Carlberg, N. De Lee, J. Johnson, H. Lewis, S. R. Majewski, M. Pinsonneault, J. Sobeck, K. G. Stassun, G. S. Stringfellow, and G. Zasowski: 2018, 'Stellar Multiplicity Meets Stellar Evolution and Metallicity: The APOGEE View'. *Astrophys. J.* **854**(2), 147.

Bear, E. and N. Soker: 2017, 'Planetary Nebulae that Cannot Be Explained by Binary Systems'. *Astrophys. J. Lett.* **837**(1), L10.

Belczynski, K., V. Kalogera, and T. Bulik: 2002, 'A Comprehensive Study of Binary Compact Objects as Gravitational Wave Sources: Evolutionary Channels, Rates, and Physical Properties'. *Astrophys. J.* **572**(1), 407–431.

Bilinski, C., N. Smith, G. G. Williams, P. Smith, J. Andrews, K. I. Clubb, W. Zheng, A. V. Filippenko, O. D. Fox, G. Hosseinzadeh, D. A. Howell, P. L. Kelly, P. Milne, D. J. Sand, J. L. Hoffman, D. C. Leonard, S. Cargill, C. Casper, G. Halevy, H. Kim, S. Kumar, K. Pina, and H. Yuk: 2020, 'SN 2014ab: an aspherical Type IIn supernova with low polarization'. *MNRAS* **498**(3), 3835–3851.

Blagorodnova, N., J. Klencki, O. Pejcha, P. M. Vreeswijk, H. E. Bond, K. B. Burdge, K. De, C. Fremling, R. D. Gehrz, J. E. Jencson, M. M. Kasliwal, T. Kupfer, R. M. Lau, F. J. Masci, and M. R. Rich: 2021, 'The luminous red nova AT 2018bwo in NGC 45 and its binary yellow

supergiant progenitor'. *arXiv e-prints* p. arXiv:2102.05662.

Brown, N. J., E. O. Waagen, C. Scovil, P. Nelson, A. Oksanen, J. Solonen, and A. Price: 2002, 'Peculiar variable in Monoceros.'. *IAU Circ.* **7785**, 1.

Burrows, A. and J. Goshy: 1993, 'A Theory of Supernova Explosions'. *Astrophys. J. Lett.* **416**, L75.

Burrows, A., D. Radice, D. Vartanyan, H. Nagakura, M. A. Skinner, and J. C. Dolence: 2020, 'The overarching framework of core-collapse supernova explosions as revealed by 3D FORNAX simulations'. *MNRAS* **491**(2), 2715–2735.

Burrows, A. and D. Vartanyan: 2021, 'Core-collapse supernova explosion theory'. *Nature* **589**(7840), 29–39.

Carroll, B. W. and D. A. Ostlie: 2007, *An introduction to modern astrophysics; 2nd ed.* San Francisco, CA: Addison-Wesley.

Chen, K.-J., A. Heger, S. Woosley, A. Almgren, D. J. Whalen, and J. L. Johnson: 2014, 'The General Relativistic Instability Supernova of a Supermassive Population III Star'. *Astrophys. J.* **790**(2), 162.

Chomiuk, L., J. D. Linford, J. Yang, T. J. O'Brien, Z. Paragi, A. J. Mioduszewski, R. J. Beswick, C. C. Cheung, K. Mukai, T. Nelson, V. A. R. M. Ribeiro, M. P. Rupen, J. L. Sokoloski, J. Weston, Y. Zheng, M. F. Bode, S. Eyres, N. Roy, and G. B. Taylor: 2014, 'Binary orbits as the driver of γ-ray emission and mass ejection in classical novae'. *Nature* **514**(7522), 339–342.

Chomiuk, L., B. D. Metzger, and K. J. Shen: 2020, 'New Insights into Classical Novae'. *arXiv e-prints* p. arXiv:2011.08751.

Clayton, M., P. Podsiadlowski, N. Ivanova, and S. Justham: 2017, 'Episodic mass ejections from common-envelope objects'. *MNRAS* **470**(2), 1788–1808.

Couch, S. M., M. L. Warren, and E. P. O'Connor: 2020, 'Simulating Turbulence-aided Neutrino-driven Core-collapse Supernova Explosions in One Dimension'. *Astrophys. J.* **890**(2), 127.

Curtis, S., K. Ebinger, C. Fröhlich, M. Hempel, A. Perego, M. Liebendörfer, and F.-K. Thielemann: 2019, 'PUSHing Core-collapse Supernovae to Explosions in Spherical Symmetry. III. Nucleosynthesis Yields'. *Astrophys. J.* **870**(1), 2.

De Marco, O.: 2009, 'The Origin and Shaping of Planetary Nebulae: Putting the Binary Hypothesis to the Test'. *Pub. of Astron. Soc. of Pacific* **121**(878), 316.

De Marco, O., J.-C. Passy, M. Moe, F. Herwig, M.-M. Mac Low, and B. Paxton: 2011, 'On the α formalism for the common envelope interaction'. *MNRAS* **411**(4), 2277–2292.

Dessart, L. and D. J. Hillier: 2019, 'The difficulty of inferring progenitor masses from type-II-Plateau supernova light curves'. *Astron. Astrophys.* **625**, A9.

Dessart, L. and D. J. Hillier: 2020, 'Radiative-transfer modeling of nebular-phase type II supernovae. Dependencies on progenitor and explosion properties'. *Astron. Astrophys.* **642**, A33.

Dominik, M., K. Belczynski, C. Fryer, D. E. Holz, E. Berti, T. Bulik, I. Mandel, and R. O'Shaughnessy: 2012, 'Double Compact Objects. I. The Significance of the Common Envelope on Merger Rates'. *Astrophys. J.* **759**(1), 52.

Ebinger, K., S. Curtis, C. Fröhlich, M. Hempel, A. Perego, M. Liebendörfer, and F.-K. Thielemann: 2019, 'PUSHing Core-collapse Supernovae to Explosions in Spherical Symmetry. II. Explodability and Remnant Properties'. *Astrophys. J.* **870**(1), 1.

Ebinger, K., S. Curtis, S. Ghosh, C. Fröhlich, M. Hempel, A. Perego, M. Liebendörfer, and F.-K. Thielemann: 2020, 'PUSHing Core-collapse Supernovae to Explosions in Spherical Symmetry. IV. Explodability, Remnant Properties, and Nucleosynthesis Yields of Low-metallicity Stars'. *Astrophys. J.* **888**(2), 91.

Eggleton, P. P. and L. Kiseleva-Eggleton: 2001, 'Orbital Evolution in Binary and Triple Stars, with an Application to SS Lacertae'. *Astrophys. J.* **562**(2), 1012–1030.

Eldridge, J. J., N. Y. Guo, N. Rodrigues, E. R. Stanway, and L. Xiao: 2019, 'Supernova lightCURVE POPulation Synthesis II: Validation against supernovae with an observed progenitor'. *Pub. of Astron. Soc. of Australia* **36**, e041.

Eldridge, J. J., E. R. Stanway, L. Xiao, L. A. S. McClelland, G. Taylor, M. Ng, S. M. L. Greis, and J. C. Bray: 2017, 'Binary Population and Spectral Synthesis Version 2.1: Construction, Observational Verification, and New Results'. *Pub. of Astron. Soc. of Australia* **34**, e058.

Ertl, T., H. T. Janka, S. E. Woosley, T. Sukhbold, and M. Ugliano: 2016, 'A Two-parameter Criterion for Classifying the Explodability of Massive Stars by the Neutrino-driven Mechanism'. *Astrophys. J.* **818**(2), 124.

Ertl, T., S. E. Woosley, T. Sukhbold, and H. T. Janka: 2020, 'The Explosion of Helium Stars Evolved with Mass Loss'. *Astrophys. J.* **890**(1), 51.

Faran, T., D. Poznanski, A. V. Filippenko, R. Chornock, R. J. Foley, M. Ganeshalingam, D. C. Leonard, W. Li, M. Modjaz, F. J. D. Serduke, and J. M. Silverman: 2014, 'A sample of Type II-L supernovae'. *MNRAS* **445**(1), 554–569.

Filippenko, A. V.: 1997, 'Optical Spectra of Supernovae'. *Annual Rev. of Astron. and Astrophys.* **35**, 309–355.

Fryer, C. L. and A. Heger: 2005, 'Binary Merger Progenitors for Gamma-Ray Bursts and Hypernovae'. *Astrophys. J.* **623**(1), 302–313.

Fryxell, B. A. and R. E. Taam: 1988, 'Numerical Simulations of Nonaxisymmetric Adiabatic Accretion Flow'. *Astrophys. J.* **335**, 862.

Glanz, H. and H. B. Perets: 2018, 'Efficient common-envelope ejection through dust-driven winds'. *MNRAS* **478**(1), L12–L17.

Glanz, H. and H. B. Perets: 2021, 'Simulations of common envelope evolution in triple systems: circumstellar case'. *MNRAS* **500**(2), 1921–1932.

Glebbeek, E., E. Gaburov, S. E. de Mink, O. R. Pols, and S. F. Portegies Zwart: 2009, 'The evolution of runaway stellar collision products'. *Astron. Astrophys.* **497**(1), 255–264.

Goldberg, J. A. and L. Bildsten: 2020, 'The Value of Progenitor Radius Measurements for Explosion Modeling of Type II-Plateau Supernovae'. *Astrophys. J. Lett.* **895**(2), L45.

Goldberg, J. A., L. Bildsten, and B. Paxton: 2019, 'Inferring Explosion Properties from Type II-Plateau Supernova Light Curves'. *Astrophys. J.* **879**(1), 3.

Gomel, R., S. Faigler, and T. Mazeh: 2021, 'Search for dormant black holes in ellipsoidal variables I. Revisiting the expected amplitudes of the photometric modulation'. *MNRAS* **501**(2), 2822–2832.

Grichener, A., E. Sabach, and N. Soker: 2018, 'The limited role of recombination energy in common envelope removal'. *MNRAS* **478**(2), 1818–1824.

Hamuy, M.: 2003, 'Observed and Physical Properties of Core-Collapse Supernovae'. *Astrophys. J.* **582**(2), 905–914.

Hirai, R., P. Podsiadlowski, S. P. Owocki, F. R. N. Schneider, and N. Smith: 2021, 'Simulating the formation of η Carinae's surrounding nebula through unstable triple evolution and stellar merger-induced eruption'. *MNRAS* **503**(3), 4276–4296.

Holoien, T. W. S., J. L. Prieto, O. Pejcha, K. Z. Stanek, C. S. Kochanek, B. J. Shappee, D. Grupe, N. Morrell, J. R. Thorstensen, U. Basu, J. F. Beacom, D. Bersier, J. Brimacombe, A. B. Davis, G. Pojmański, and D. M. Skowron: 2016, 'Discovery and Observations of the Unusually Luminous Type-Defying II-P/II-L Supernova ASASSN-13co'. *Acta Astron.* **66**(2),

219–238.

Hubová, D. and O. Pejcha: 2019, 'Kinematics of mass-loss from the outer Lagrange point L2'. *MNRAS* **489**(1), 891–899.

Iben, Icko, J. and M. Livio: 1993, 'Common Envelopes in Binary Star Evolution'. *Pub. of Astron. Soc. of Pacific* **105**, 1373.

Ivanova, N. and S. Chaichenets: 2011, 'Common Envelope: Enthalpy Consideration'. *Astrophys. J. Lett.* **731**(2), L36.

Ivanova, N., S. Justham, J. L. Avendano Nandez, and J. C. Lombardi: 2013a, 'Identification of the Long-Sought Common-Envelope Events'. *Science* **339**(6118), 433.

Ivanova, N., S. Justham, X. Chen, O. De Marco, C. L. Fryer, E. Gaburov, H. Ge, E. Glebbeek, Z. Han, X. D. Li, G. Lu, T. Marsh, P. Podsiadlowski, A. Potter, N. Soker, R. Taam, T. M. Tauris, E. P. J. van den Heuvel, and R. F. Webbink: 2013b, 'Common envelope evolution: where we stand and how we can move forward'. *Astron. and Astroph. Rev.* **21**, 59.

Ivanova, N., S. Justham, and P. Podsiadlowski: 2015, 'On the role of recombination in common-envelope ejections'. *MNRAS* **447**(3), 2181–2197.

Janka, H.-T., T. Melson, and A. Summa: 2016, 'Physics of Core-Collapse Supernovae in Three Dimensions: A Sneak Preview'. *Annual Review of Nuclear and Particle Science* **66**(1), 341–375.

Jayasinghe, T., C. S. Kochanek, K. Z. Stanek, B. J. Shappee, T. W. S. Holoien, T. A. Thompson, J. L. Prieto, S. Dong, M. Pawlak, O. Pejcha, G. Pojmanski, S. Otero, N. Hurst, and D. Will: 2021a, 'The ASAS-SN catalogue of variable stars IX: The spectroscopic properties of Galactic variable stars'. *MNRAS* **503**(1), 200–235.

Jayasinghe, T., K. Z. Stanek, C. S. Kochanek, B. J. Shappee, T. W. S. Holoien, T. A. Thompson, J. L. Prieto, S. Dong, M. Pawlak, O. Pejcha, J. V. Shields, G. Pojmanski, S. Otero, C. A. Britt, and D. Will: 2019a, 'The ASAS-SN catalogue of variable stars - II. Uniform classification of 412 000 known variables'. *MNRAS* **486**(2), 1907–1943.

Jayasinghe, T., K. Z. Stanek, C. S. Kochanek, B. J. Shappee, T. W. S. Holoien, T. A. Thompson, J. L. Prieto, S. Dong, M. Pawlak, O. Pejcha, J. V. Shields, G. Pojmanski, S. Otero, N. Hurst, C. A. Britt, and D. Will: 2019b, 'The ASAS-SN catalogue of variable stars III: variables in the southern TESS continuous viewing zone'. *MNRAS* **485**(1), 961–971.

Jayasinghe, T., K. Z. Stanek, C. S. Kochanek, B. J. Shappee, T. W. S. Holoien, T. A. Thompson, J. L. Prieto, S. Dong, M. Pawlak, O. Pejcha, J. V. Shields, G. Pojmanski, S. Otero, N. Hurst, C. A. Britt, and D. Will: 2020a, 'The ASAS-SN catalogue of variable stars - V. Variables in the Southern hemisphere'. *MNRAS* **491**(1), 13–28.

Jayasinghe, T., K. Z. Stanek, C. S. Kochanek, B. J. Shappee, M. H. Pinsonneault, T. W. S. Holoien, T. A. Thompson, J. L. Prieto, M. Pawlak, O. Pejcha, G. Pojmanski, S. Otero, N. Hurst, and D. Will: 2020b, 'The ASAS-SN catalogue of variable stars - VII. Contact binaries are different above and below the Kraft break'. *MNRAS* **493**(3), 4045–4057.

Jayasinghe, T., K. Z. Stanek, C. S. Kochanek, P. J. Vallely, B. J. Shappee, T. W. S. Holoien, T. A. Thompson, J. L. Prieto, O. Pejcha, M. Fausnaugh, S. Otero, N. Hurst, and D. Will: 2020c, 'The ASAS-SN catalogue of variable stars VI: an all-sky sample of δ Scuti stars'. *MNRAS* **493**(3), 4186–4208.

Jayasinghe, T., K. Z. Stanek, T. A. Thompson, C. S. Kochanek, D. M. Rowan, P. J. Vallely, K. G. Strassmeier, M. Weber, J. T. Hinkle, F. J. Hambsch, D. Martin, J. L. Prieto, T. Pessi, D. Huber, K. Auchettl, L. A. Lopez, I. Ilyin, C. Badenes, A. W. Howard, H. Isaacson, and S. J. Murphy: 2021b, 'A Unicorn in Monoceros: the $3M_\odot$ dark companion to the bright, nearby red giant V723 Mon is a non-interacting, mass-gap black hole candidate'. *arXiv e-prints* p.

arXiv:2101.02212.

Jones, D. and H. M. J. Boffin: 2017, 'Binary stars as the key to understanding planetary nebulae'. *Nature Astronomy* **1**, 0117.

Jones, D., O. Pejcha, and R. L. M. Corradi: 2019, 'On the triple-star origin of the planetary nebula Sh 2-71'. *MNRAS* **489**(2), 2195–2203.

Kasen, D. and S. E. Woosley: 2009, 'Type II Supernovae: Model Light Curves and Standard Candle Relationships'. *Astrophys. J.* **703**(2), 2205–2216.

Kashi, A. and N. Soker: 2010, 'Common Powering Mechanism of Intermediate Luminosity Optical Transients and Luminous Blue Variables'. *arXiv e-prints* p. arXiv:1011.1222.

Kasliwal, M. M., J. Bally, F. Masci, A. M. Cody, H. E. Bond, J. E. Jencson, S. Tinyanont, Y. Cao, C. Contreras, D. A. Dykhoff, S. Amodeo, L. Armus, M. Boyer, M. Cantiello, R. L. Carlon, A. C. Cass, D. Cook, D. T. Corgan, J. Faella, O. D. Fox, W. Green, R. D. Gehrz, G. Helou, E. Hsiao, J. Johansson, R. M. Khan, R. M. Lau, N. Langer, E. Levesque, P. Milne, S. Mohamed, N. Morrell, A. Monson, A. Moore, E. O. Ofek, D. O' Sullivan, M. Parthasarathy, A. Perez, D. A. Perley, M. Phillips, T. A. Prince, D. Shenoy, N. Smith, J. Surace, S. D. Van Dyk, P. A. Whitelock, and R. Williams: 2017, 'SPIRITS: Uncovering Unusual Infrared Transients with Spitzer'. *Astrophys. J.* **839**(2), 88.

Katz, B. and S. Dong: 2012, 'The rate of WD-WD head-on collisions may be as high as the SNe Ia rate'. *arXiv e-prints* p. arXiv:1211.4584.

Kirshner, R. P. and J. Kwan: 1974, 'Distances to extragalactic supernovae.'. *Astrophys. J.* **193**, 27–36.

Kochanek, C. S.: 2019, 'The physics of flash (supernova) spectroscopy'. *MNRAS* **483**(3), 3762–3772.

Kochanek, C. S., S. M. Adams, and K. Belczynski: 2014, 'Stellar mergers are common'. *MNRAS* **443**(2), 1319–1328.

Kochanek, C. S., B. J. Shappee, K. Z. Stanek, T. W. S. Holoien, T. A. Thompson, J. L. Prieto, S. Dong, J. V. Shields, D. Will, C. Britt, D. Perzanowski, and G. Pojmański: 2017, 'The All-Sky Automated Survey for Supernovae (ASAS-SN) Light Curve Server v1.0'. *Pub. of Astron. Soc. of Pacific* **129**(980), 104502.

Kreidberg, L., C. D. Bailyn, W. M. Farr, and V. Kalogera: 2012, 'Mass Measurements of Black Holes in X-Ray Transients: Is There a Mass Gap?'. *Astrophys. J.* **757**(1), 36.

Kuiper, G. P.: 1941, 'On the Interpretation of β Lyrae and Other Close Binaries.'. *Astrophys. J.* **93**, 133.

Kurfürst, P. and J. Krtička: 2019, 'Modeling of interactions between supernovae ejecta and aspherical circumstellar environments'. *Astron. Astrophys.* **625**, A24.

Kurfürst, P., O. Pejcha, and J. Krtička: 2020, 'Supernova explosions interacting with aspherical circumstellar material: implications for light curves, spectral line profiles, and polarization'. *Astron. Astrophys.* **642**, A214.

Kushnir, D. and B. Katz: 2015, 'Failure of a Neutrino-driven Explosion after Core-collapse May Lead to a Thermonuclear Supernova'. *Astrophys. J.* **811**(2), 97.

Li, K.-L., B. D. Metzger, L. Chomiuk, I. Vurm, J. Strader, T. Finzell, A. M. Beloborodov, T. Nelson, B. J. Shappee, C. S. Kochanek, J. L. Prieto, S. Kafka, T. W. S. Holoien, T. A. Thompson, P. J. Luckas, and H. Itoh: 2017, 'A nova outburst powered by shocks'. *Nature Astronomy* **1**, 697–702.

Lipunov, V. M., S. Blinnikov, E. Gorbovskoy, A. Tutukov, P. Baklanov, V. Krushinski, N. Tiurina, P. Balanutsa, A. Kuznetsov, V. Kornilov, I. Gorbunov, V. Shumkov, V. Vladimirov,

O. Gress, N. M. Budnev, K. Ivanov, A. Tlatov, A. Gabovich, V. Yurkov, Y. Sergienko, and I. Zalozhnykh: 2017, 'MASTER OT J004207.99+405501.1/M31LRN 2015 luminous red nova in M31: discovery, light curve, hydrodynamics and evolution'. *MNRAS* **470**(2), 2339–2350.

Litvinova, I. Y. and D. K. Nadezhin: 1985, 'Determination of Integrated Parameters for Type-II Supernovae'. *Soviet Astronomy Letters* **11**, 145–147.

Livio, M. and N. Soker: 1988, 'The Common Envelope Phase in the Evolution of Binary Stars'. *Astrophys. J.* **329**, 764.

Lovegrove, E. and S. E. Woosley: 2013, 'Very Low Energy Supernovae from Neutrino Mass Loss'. *Astrophys. J.* **769**(2), 109.

LSST Science Collaboration: 2009, 'LSST Science Book, Version 2.0'. *arXiv e-prints* p. arXiv:0912.0201.

Mabanta, Q. A., J. W. Murphy, and J. C. Dolence: 2019, 'Convection-aided Explosions in One-dimensional Core-collapse Supernova Simulations. I. Technique and Validation'. *Astrophys. J.* **887**(1), 43.

MacLeod, M., P. Macias, E. Ramirez-Ruiz, J. Grindlay, A. Batta, and G. Montes: 2017, 'Lessons from the Onset of a Common Envelope Episode: the Remarkable M31 2015 Luminous Red Nova Outburst'. *Astrophys. J.* **835**(2), 282.

MacLeod, M. and E. Ramirez-Ruiz: 2015, 'Asymmetric Accretion Flows within a Common Envelope'. *Astrophys. J.* **803**(1), 41.

Majewski, S. R., R. P. Schiavon, P. M. Frinchaboy, C. Allende Prieto, R. Barkhouser, D. Bizyaev, B. Blank, S. Brunner, A. Burton, R. Carrera, S. D. Chojnowski, K. Cunha, C. Epstein, G. Fitzgerald, A. E. García Pérez, F. R. Hearty, C. Henderson, J. A. Holtzman, J. A. Johnson, C. R. Lam, J. E. Lawler, P. Maseman, S. Mészáros, M. Nelson, D. C. Nguyen, D. L. Nidever, M. Pinsonneault, M. Shetrone, S. Smee, V. V. Smith, T. Stolberg, M. F. Skrutskie, E. Walker, J. C. Wilson, G. Zasowski, F. Anders, S. Basu, S. Beland, M. R. Blanton, J. Bovy, J. R. Brownstein, J. Carlberg, W. Chaplin, C. Chiappini, D. J. Eisenstein, Y. Elsworth, D. Feuillet, S. W. Fleming, J. Galbraith-Frew, R. A. García, D. A. García-Hernández, B. A. Gillespie, L. Girardi, J. E. Gunn, S. Hasselquist, M. R. Hayden, S. Hekker, I. Ivans, K. Kinemuchi, M. Klaene, S. Mahadevan, S. Mathur, B. Mosser, D. Muna, J. A. Munn, R. C. Nichol, R. W. O'Connell, J. K. Parejko, A. C. Robin, H. Rocha-Pinto, M. Schultheis, A. M. Serenelli, N. Shane, V. Silva Aguirre, J. S. Sobeck, B. Thompson, N. W. Troup, D. H. Weinberg, and O. Zamora: 2017, 'The Apache Point Observatory Galactic Evolution Experiment (APOGEE)'. *Astronom. J.* **154**(3), 94.

Margutti, R., B. D. Metzger, R. Chornock, I. Vurm, N. Roth, B. W. Grefenstette, V. Savchenko, R. Cartier, J. F. Steiner, G. Terreran, B. Margalit, G. Migliori, D. Milisavljevic, K. D. Alexander, M. Bietenholz, P. K. Blanchard, E. Bozzo, D. Brethauer, I. V. Chilingarian, D. L. Coppejans, L. Ducci, C. Ferrigno, W. Fong, D. Götz, C. Guidorzi, A. Hajela, K. Hurley, E. Kuulkers, P. Laurent, S. Mereghetti, M. Nicholl, D. Patnaude, P. Ubertini, J. Banovetz, N. Bartel, E. Berger, E. R. Coughlin, T. Eftekhari, D. D. Frederiks, A. V. Kozlova, T. Laskar, D. S. Svinkin, M. R. Drout, A. MacFadyen, and K. Paterson: 2019, 'An Embedded X-Ray Source Shines through the Aspherical AT 2018cow: Revealing the Inner Workings of the Most Luminous Fast-evolving Optical Transients'. *Astrophys. J.* **872**(1), 18.

Martini, P., R. M. Wagner, A. Tomaney, R. M. Rich, M. della Valle, and P. H. Hauschildt: 1999, 'Nova Sagittarii 1994 1 (V4332 Sagittarii): The Discovery and Evolution of an Unusual Luminous Red Variable Star'. *Astronom. J.* **118**(2), 1034–1042.

Mason, E., M. Diaz, R. E. Williams, G. Preston, and T. Bensby: 2010, 'The peculiar nova V1309 Scorpii/nova Scorpii 2008. A candidate twin of V838 Monocerotis'. *Astron. Astrophys.* **516**,

A108.

Masuda, K. and T. Hirano: 2021, 'Tidal Effects on the Radial Velocities of V723 Mon: Additional Evidence for a Dark 3 $M_\odot$ Companion'. *Astrophys. J. Lett.* **910**(2), L17.

Mauerhan, J. C., N. Smith, A. V. Filippenko, K. B. Blanchard, P. K. Blanchard, C. F. E. Casper, S. B. Cenko, K. I. Clubb, D. P. Cohen, K. L. Fuller, G. Z. Li, and J. M. Silverman: 2013a, 'The unprecedented 2012 outburst of SN 2009ip: a luminous blue variable star becomes a true supernova'. *MNRAS* **430**(3), 1801–1810.

Mauerhan, J. C., N. Smith, J. M. Silverman, A. V. Filippenko, A. N. Morgan, S. B. Cenko, M. Ganeshalingam, K. I. Clubb, J. S. Bloom, T. Matheson, and P. Milne: 2013b, 'SN 2011ht: confirming a class of interacting supernovae with plateau light curves (Type IIn-P)'. *MNRAS* **431**(3), 2599–2611.

McDowell, A. T., P. C. Duffell, and D. Kasen: 2018, 'Interaction of a Supernova with a Circumstellar Disk'. *Astrophys. J.* **856**(1), 29.

Metzger, B. D. and O. Pejcha: 2017, 'Shock-powered light curves of luminous red novae as signatures of pre-dynamical mass-loss in stellar mergers'. *MNRAS* **471**(3), 3200–3211.

Meyer, F. and E. Meyer-Hofmeister: 1979, 'Formation of cataclysmic binaries through common envelope evolution.'. *Astron. Astrophys.* **78**, 167–176.

Mikulášek, Z., A. Skopal, M. Zejda, O. Pejcha, L. Kohoutek, D. Motl, A. A. Vittone, and L. Errico: 2007, 'Light Variations of the Anomalous Central Star of Planetary Nebula Sh 2-71'. In: A. T. Okazaki, S. P. Owocki, and S. Stefl (eds.): *Active OB-Stars: Laboratories for Stellare and Circumstellar Physics*, Vol. 361 of *Astronomical Society of the Pacific Conference Series*. p. 469.

Miller, A., M. Kounkel, C. Boggio, K. Covey, and A. M. Price-Whelan: 2021, 'Orbital and Stellar Parameters for 2M06464003+0109157: A Double-lined Eclipsing Binary of Spotted, Sub-solar Twins'. *Pub. of Astron. Soc. of Pacific* **133**(1022), 044201.

Moe, M. and R. Di Stefano: 2017, 'Mind Your Ps and Qs: The Interrelation between Period (P) and Mass-ratio (Q) Distributions of Binary Stars'. *Astrophys. J., Suppl. Ser.* **230**(2), 15.

Moe, M., K. M. Kratter, and C. Badenes: 2019, 'The Close Binary Fraction of Solar-type Stars Is Strongly Anticorrelated with Metallicity'. *Astrophys. J.* **875**(1), 61.

Morozova, V., A. L. Piro, and S. Valenti: 2017, 'Unifying Type II Supernova Light Curves with Dense Circumstellar Material'. *Astrophys. J.* **838**(1), 28.

Morozova, V., A. L. Piro, and S. Valenti: 2018, 'Measuring the Progenitor Masses and Dense Circumstellar Material of Type II Supernovae'. *Astrophys. J.* **858**(1), 15.

Morris, T. and P. Podsiadlowski: 2007, 'The Triple-Ring Nebula Around SN 1987A: Fingerprint of a Binary Merger'. *Science* **315**(5815), 1103.

Mould, J., J. Cohen, J. R. Graham, D. Hamilton, K. Matthews, A. Picard, N. Reid, M. Schmidt, T. Soifer, C. Wilson, R. M. Rich, and J. Gunn: 1990, 'A Nova-like Red Variable in M31'. *Astrophys. J. Lett.* **353**, L35.

Močnik, T., M. Lloyd, D. Pollacco, and R. A. Street: 2015, 'The central star candidate of the planetary nebula Sh2-71: photometric and spectroscopic variability'. *MNRAS* **451**(1), 870–877.

Müller, B.: 2020, 'Hydrodynamics of core-collapse supernovae and their progenitors'. *Living Reviews in Computational Astrophysics* **6**(1), 3.

Müller, B., A. Heger, D. Liptai, and J. B. Cameron: 2016, 'A simple approach to the supernova progenitor-explosion connection'. *MNRAS* **460**(1), 742–764.

Müller, T., J. L. Prieto, O. Pejcha, and A. Clocchiatti: 2017, 'The Nickel Mass Distribution of

Normal Type II Supernovae'. *Astrophys. J.* **841**(2), 127.

Munari, U., A. Henden, S. Kiyota, D. Laney, F. Marang, T. Zwitter, R. L. M. Corradi, S. Desidera, P. M. Marrese, E. Giro, F. Boschi, and M. B. Schwartz: 2002, 'The mysterious eruption of V838 Mon'. *Astron. Astrophys.* **389**, L51–L56.

Nagy, A. P., A. Ordasi, J. Vinkó, and J. C. Wheeler: 2014, 'A semianalytical light curve model and its application to type IIP supernovae'. *Astron. Astrophys.* **571**, A77.

Nakamura, K., T. Takiwaki, T. Kuroda, and K. Kotake: 2015, 'Systematic features of axisymmetric neutrino-driven core-collapse supernova models in multiple progenitors'. *Pub. of Astron. Soc. of Japan* **67**(6), 107.

Nandez, J. L. A., N. Ivanova, and J. Lombardi, J. C.: 2014, 'V1309 Sco—Understanding a Merger'. *Astrophys. J.* **786**(1), 39.

Nandez, J. L. A., N. Ivanova, and J. C. J. Lombardi: 2015, 'Recombination energy in double white dwarf formation.'. *MNRAS* **450**, L39–L43.

Naoz, S. and D. C. Fabrycky: 2014, 'Mergers and Obliquities in Stellar Triples'. *Astrophys. J.* **793**(2), 137.

Nelemans, G., F. Verbunt, L. R. Yungelson, and S. F. Portegies Zwart: 2000, 'Reconstructing the evolution of double helium white dwarfs: envelope loss without spiral-in'. *Astron. Astrophys.* **360**, 1011–1018.

O'Connor, E. and C. D. Ott: 2010, 'A new open-source code for spherically symmetric stellar collapse to neutron stars and black holes'. *Classical and Quantum Gravity* **27**(11), 114103.

O'Connor, E. and C. D. Ott: 2011, 'Black Hole Formation in Failing Core-Collapse Supernovae'. *Astrophys. J.* **730**(2), 70.

Ohlmann, S. T., F. K. Röpke, R. Pakmor, and V. Springel: 2016, 'Hydrodynamic Moving-mesh Simulations of the Common Envelope Phase in Binary Stellar Systems'. *Astrophys. J. Lett.* **816**(1), L9.

Özel, F. and P. Freire: 2016, 'Masses, Radii, and the Equation of State of Neutron Stars'. *Annual Rev. of Astron. and Astrophys.* **54**, 401–440.

Özel, F., D. Psaltis, R. Narayan, and J. E. McClintock: 2010, 'The Black Hole Mass Distribution in the Galaxy'. *Astrophys. J.* **725**(2), 1918–1927.

Paczynski, B.: 1976, 'Common Envelope Binaries'. In: P. Eggleton, S. Mitton, and J. Whelan (eds.): *Structure and Evolution of Close Binary Systems*, Vol. 73. p. 75.

Papish, O. and N. Soker: 2011, 'Exploding core collapse supernovae with jittering jets'. *MNRAS* **416**(3), 1697–1702.

Papish, O., N. Soker, and I. Bukay: 2015, 'Ejecting the envelope of red supergiant stars with jets launched by an inspiralling neutron star'. *MNRAS* **449**(1), 288–295.

Pastorello, A. and M. Fraser: 2019, 'Supernova impostors and other gap transients'. *Nature Astronomy* **3**, 676–679.

Pastorello, A., E. Mason, S. Taubenberger, M. Fraser, G. Cortini, L. Tomasella, M. T. Botticella, N. Elias-Rosa, R. Kotak, S. J. Smartt, S. Benetti, E. Cappellaro, M. Turatto, L. Tartaglia, S. G. Djorgovski, A. J. Drake, M. Berton, F. Briganti, J. Brimacombe, F. Bufano, Y. Z. Cai, S. Chen, E. J. Christensen, F. Ciabattari, E. Congiu, A. Dimai, C. Inserra, E. Kankare, L. Magill, K. Maguire, F. Martinelli, A. Morales-Garoffolo, P. Ochner, G. Pignata, A. Reguitti, J. Sollerman, S. Spiro, G. Terreran, and D. E. Wright: 2019, 'Luminous red novae: Stellar mergers or giant eruptions?'. *Astron. Astrophys.* **630**, A75.

Patton, R. A. and T. Sukhbold: 2020, 'Towards a realistic explosion landscape for binary population synthesis'. *MNRAS* **499**(2), 2803–2816.

Pawlak, M., O. Pejcha, P. Jakubčík, T. Jayasinghe, C. S. Kochanek, K. Z. Stanek, B. J. Shappee, T. W. S. Holoien, T. A. Thompson, J. L. Prieto, S. Dong, J. V. Shields, G. Pojmanski, C. A. Britt, and D. Will: 2019, 'The ASAS-SN catalogue of variable stars - IV. Periodic variables in the APOGEE survey'. *MNRAS* **487**(4), 5932–5945.

Pejcha, O.: 2014, 'Burying a Binary: Dynamical Mass Loss and a Continuous Optically thick Outflow Explain the Candidate Stellar Merger V1309 Scorpii'. *Astrophys. J.* **788**(1), 22.

Pejcha, O.: 2020, 'The Explosion Mechanism of Core-Collapse Supernovae and Its Observational Signatures'. In: P. Kabáth, D. Jones, and M. Skarka (eds.): *Reviews in Frontiers of Modern Astrophysics; From Space Debris to Cosmology.* Cham: Springer International Publishing, pp. 189–211.

Pejcha, O., J. M. Antognini, B. J. Shappee, and T. A. Thompson: 2013, 'Greatly enhanced eccentricity oscillations in quadruple systems composed of two binaries: implications for stars, planets and transients'. *MNRAS* **435**(2), 943–951.

Pejcha, O., B. Dasgupta, and T. A. Thompson: 2012a, 'Effect of collective neutrino oscillations on the neutrino mechanism of core-collapse supernovae'. *MNRAS* **425**(2), 1083–1090.

Pejcha, O., B. D. Metzger, and K. Tomida: 2016a, 'Cool and luminous transients from mass-losing binary stars'. *MNRAS* **455**(4), 4351–4372.

Pejcha, O., B. D. Metzger, and K. Tomida: 2016b, 'Binary stellar mergers with marginally bound ejecta: excretion discs, inflated envelopes, outflows, and their luminous transients'. *MNRAS* **461**(3), 2527–2539.

Pejcha, O., B. D. Metzger, J. G. Tyles, and K. Tomida: 2017, 'Pre-explosion Spiral Mass Loss of a Binary Star Merger'. *Astrophys. J.* **850**(1), 59.

Pejcha, O. and J. L. Prieto: 2015a, 'A Global Model of The Light Curves and Expansion Velocities of Type II-plateau Supernovae'. *Astrophys. J.* **799**(2), 215.

Pejcha, O. and J. L. Prieto: 2015b, 'On the Intrinsic Diversity of Type II-Plateau Supernovae'. *Astrophys. J.* **806**(2), 225.

Pejcha, O. and T. A. Thompson: 2012, 'The Physics of the Neutrino Mechanism of Core-collapse Supernovae'. *Astrophys. J.* **746**(1), 106.

Pejcha, O. and T. A. Thompson: 2015, 'The Landscape of the Neutrino Mechanism of Core-collapse Supernovae: Neutron Star and Black Hole Mass Functions, Explosion Energies, and Nickel Yields'. *Astrophys. J.* **801**(2), 90.

Pejcha, O., T. A. Thompson, and C. S. Kochanek: 2012b, 'The observed neutron star mass distribution as a probe of the supernova explosion mechanism'. *MNRAS* **424**(2), 1570–1583.

Perego, A., M. Hempel, C. Fröhlich, K. Ebinger, M. Eichler, J. Casanova, M. Liebendörfer, and F. K. Thielemann: 2015, 'PUSHing Core-collapse Supernovae to Explosions in Spherical Symmetry I: the Model and the Case of SN 1987A'. *Astrophys. J.* **806**(2), 275.

Popov, D. V.: 1993, 'An Analytical Model for the Plateau Stage of Type II Supernovae'. *Astrophys. J.* **414**, 712.

Portegies Zwart, S. F. and E. P. J. van den Heuvel: 2016, 'Was the nineteenth century giant eruption of Eta Carinae a merger event in a triple system?'. *MNRAS* **456**(4), 3401–3412.

Pumo, M. L., L. Zampieri, S. Spiro, A. Pastorello, S. Benetti, E. Cappellaro, G. Manicò, and M. Turatto: 2017, 'Radiation-hydrodynamical modelling of underluminous Type II plateau supernovae'. *MNRAS* **464**(3), 3013–3020.

Raghavan, D., H. A. McAlister, T. J. Henry, D. W. Latham, G. W. Marcy, B. D. Mason, D. R. Gies, R. J. White, and T. A. ten Brummelaar: 2010, 'A Survey of Stellar Families: Multiplicity of Solar-type Stars'. *Astrophys. J., Suppl. Ser.* **190**(1), 1–42.

Raithel, C. A., T. Sukhbold, and F. Özel: 2018, 'Confronting Models of Massive Star Evolution and Explosions with Remnant Mass Measurements'. *Astrophys. J.* **856**(1), 35.

Raives, M. J., S. M. Couch, J. P. Greco, O. Pejcha, and T. A. Thompson: 2018, 'The antesonic condition for the explosion of core-collapse supernovae - I. Spherically symmetric polytropic models: stability and wind emergence'. *MNRAS* **481**(3), 3293–3304.

Rasio, F. A.: 1995, 'The Minimum Mass Ratio of W Ursae Majoris Binaries'. *Astrophys. J. Lett.* **444**, L41.

Reichardt, T. A., O. De Marco, R. Iaconi, L. Chamandy, and D. J. Price: 2020, 'The impact of recombination energy on simulations of the common-envelope binary interaction'. *MNRAS* **494**(4), 5333–5349.

Rivinius, T., D. Baade, P. Hadrava, M. Heida, and R. Klement: 2020, 'A naked-eye triple system with a nonaccreting black hole in the inner binary'. *Astron. Astrophys.* **637**, L3.

Rucinski, S. M.: 2001, 'The Photometric Amplitude and Mass Ratio Distributions of Contact Binary Stars'. *Astronom. J.* **122**(2), 1007–1022.

Salpeter, E. E.: 1955, 'The Luminosity Function and Stellar Evolution.'. *Astrophys. J.* **121**, 161.

Sana, H., S. E. de Mink, A. de Koter, N. Langer, C. J. Evans, M. Gieles, E. Gosset, R. G. Izzard, J. B. Le Bouquin, and F. R. N. Schneider: 2012, 'Binary Interaction Dominates the Evolution of Massive Stars'. *Science* **337**(6093), 444.

Sand, C., S. T. Ohlmann, F. R. N. Schneider, R. Pakmor, and F. K. Röpke: 2020, 'Common-envelope evolution with an asymptotic giant branch star'. *Astron. Astrophys.* **644**, A60.

Schneider, F. R. N., P. Podsiadlowski, N. Langer, N. Castro, and L. Fossati: 2016, 'Rejuvenation of stellar mergers and the origin of magnetic fields in massive stars'. *MNRAS* **457**(3), 2355–2365.

Schreier, R., S. Hillel, and N. Soker: 2019, 'Inclined jets inside a common envelope of a triple stellar system'. *MNRAS* **490**(4), 4748–4755.

Shappee, B. J., J. L. Prieto, D. Grupe, C. S. Kochanek, K. Z. Stanek, G. De Rosa, S. Mathur, Y. Zu, B. M. Peterson, R. W. Pogge, S. Komossa, M. Im, J. Jencson, T. W. S. Holoien, U. Basu, J. F. Beacom, D. M. Szczygieł, J. Brimacombe, S. Adams, A. Campillay, C. Choi, C. Contreras, M. Dietrich, M. Dubberley, M. Elphick, S. Foale, M. Giustini, C. Gonzalez, E. Hawkins, D. A. Howell, E. Y. Hsiao, M. Koss, K. M. Leighly, N. Morrell, D. Mudd, D. Mullins, J. M. Nugent, J. Parrent, M. M. Phillips, G. Pojmanski, W. Rosing, R. Ross, D. Sand, D. M. Terndrup, S. Valenti, Z. Walker, and Y. Yoon: 2014, 'The Man behind the Curtain: X-Rays Drive the UV through NIR Variability in the 2013 Active Galactic Nucleus Outburst in NGC 2617'. *Astrophys. J.* **788**(1), 48.

Shiber, S., R. Iaconi, O. De Marco, and N. Soker: 2019, 'Companion-launched jets and their effect on the dynamics of common envelope interaction simulations'. *MNRAS* **488**(4), 5615–5632.

Shu, F. H., S. H. Lubow, and L. Anderson: 1979, 'On the structure of contact binaries. III. Mass and energy flow.'. *Astrophys. J.* **229**, 223–241.

Sills, A., J. A. Faber, J. Lombardi, James C., F. A. Rasio, and A. R. Warren: 2001, 'Evolution of Stellar Collision Products in Globular Clusters. II. Off-Axis Collisions'. *Astrophys. J.* **548**(1), 323–334.

Sills, A., J. Lombardi, James C., C. D. Bailyn, P. Demarque, F. A. Rasio, and S. L. Shapiro: 1997, 'Evolution of Stellar Collision Products in Globular Clusters. I. Head-on Collisions'. *Astrophys. J.* **487**(1), 290–303.

Silverman, J. M., S. Pickett, J. C. Wheeler, A. V. Filippenko, J. Vinkó, G. H. Marion, S. B.

Cenko, R. Chornock, K. I. Clubb, R. J. Foley, M. L. Graham, P. L. Kelly, T. Matheson, and J. C. Shields: 2017, 'After the Fall: Late-Time Spectroscopy of Type IIP Supernovae'. *MNRAS* **467**(1), 369–411.

Smith, N.: 2013, 'The Crab nebula and the class of Type IIn-P supernovae caused by sub-energetic electron-capture explosions'. *MNRAS* **434**(1), 102–113.

Smith, N.: 2017, 'Interacting Supernovae: Types IIn and Ibn'. In: A. W. Alsabti and P. Murdin (eds.): *Handbook of Supernovae*. Springer International Publishing, p. 403.

Smith, N., J. C. Mauerhan, S. B. Cenko, M. M. Kasliwal, J. M. Silverman, A. V. Filippenko, A. Gal-Yam, K. I. Clubb, M. L. Graham, D. C. Leonard, J. C. Horst, G. G. Williams, J. E. Andrews, S. R. Kulkarni, P. Nugent, M. Sullivan, K. Maguire, D. Xu, and S. Ben-Ami: 2015, 'PTF11iqb: cool supergiant mass-loss that bridges the gap between Type IIn and normal supernovae'. *MNRAS* **449**(2), 1876–1896.

Sobotka, P., L. Smelcer, O. Pejcha, L. Kral, M. Kolasa, K. Hornoch, and F. Lomoz: 2002, 'CCD Observations of the Outburst of V838 Mon'. *Information Bulletin on Variable Stars* **5336**, 1.

Soker, N. and R. Tylenda: 2003, 'Main-Sequence Stellar Eruption Model for V838 Monocerotis'. *Astrophys. J. Lett.* **582**(2), L105–L108.

Stanway, E. R. and J. J. Eldridge: 2018, 'Re-evaluating old stellar populations'. *MNRAS* **479**(1), 75–93.

Sukhbold, T., T. Ertl, S. E. Woosley, J. M. Brown, and H. T. Janka: 2016, 'Core-collapse Supernovae from 9 to 120 Solar Masses Based on Neutrino-powered Explosions'. *Astrophys. J.* **821**(1), 38.

Sukhbold, T. and S. E. Woosley: 2014, 'The Compactness of Presupernova Stellar Cores'. *Astrophys. J.* **783**(1), 10.

Sukhbold, T., S. E. Woosley, and A. Heger: 2018, 'A High-resolution Study of Presupernova Core Structure'. *Astrophys. J.* **860**(2), 93.

Suzuki, A., T. J. Moriya, and T. Takiwaki: 2019, 'Supernova Ejecta Interacting with a Circumstellar Disk. I. Two-dimensional Radiation-hydrodynamic Simulations'. *Astrophys. J.* **887**(2), 249.

Sytov, A. Y., P. V. Kaigorodov, D. V. Bisikalo, O. A. Kuznetsov, and A. A. Boyarchuk: 2007, 'The mechanism of circumbinary envelope formation in close binaries'. *Astronomy Reports* **51**(10), 836–846.

Szalai, T., J. Vinkó, R. Könyves-Tóth, A. P. Nagy, K. A. Bostroem, K. Sárneczky, P. J. Brown, O. Pejcha, A. Bódi, B. Cseh, G. Csörnyei, Z. Dencs, O. Hanyecz, B. Ignácz, C. Kalup, L. Kriskovics, A. Ordasi, A. Pál, B. Seli, Á. Sódor, R. Szakáts, K. Vida, G. Zsidi, Konkoly Team, I. Arcavi, C. Ashall, J. Burke, L. Galbany, D. Hiramatsu, G. Hosseinzadeh, E. Y. Hsiao, D. A. Howell, C. McCully, S. Moran, J. Rho, D. J. Sand, M. Shahbandeh, S. Valenti, X. Wang, J. C. Wheeler, and G. Supernova Project: 2019a, 'The Type II-P Supernova 2017eaw: From Explosion to the Nebular Phase'. *Astrophys. J.* **876**(1), 19.

Szalai, T., S. Zsíros, O. D. Fox, O. Pejcha, and T. Müller: 2019b, 'A Comprehensive Analysis of Spitzer Supernovae'. *Astrophys. J., Suppl. Ser.* **241**(2), 38.

Taam, R. E. and E. L. Sandquist: 2000, 'Common Envelope Evolution of Massive Binary Stars'. *Annual Rev. of Astron. and Astrophys.* **38**, 113–141.

Tammann, G. A., W. Loeffler, and A. Schroeder: 1994, 'The Galactic Supernova Rate'. *Astrophys. J., Suppl. Ser.* **92**, 487.

Thompson, T. A.: 2011, 'Accelerating Compact Object Mergers in Triple Systems with the Kozai Resonance: A Mechanism for "Prompt" Type Ia Supernovae, Gamma-Ray Bursts, and

Other Exotica'. *Astrophys. J.* **741**(2), 82.

Thompson, T. A., C. S. Kochanek, K. Z. Stanek, C. Badenes, R. S. Post, T. Jayasinghe, D. W. Latham, A. Bieryla, G. A. Esquerdo, P. Berlind, M. L. Calkins, J. Tayar, L. Lindegren, J. A. Johnson, T. W. S. Holoien, K. Auchettl, and K. Covey: 2019, 'A noninteracting low-mass black hole-giant star binary system'. *Science* **366**(6465), 637–640.

Timmes, F. X., S. E. Woosley, and T. A. Weaver: 1996, 'The Neutron Star and Black Hole Initial Mass Function'. *Astrophys. J.* **457**, 834.

Tylenda, R., M. Hajduk, T. Kamiński, A. Udalski, I. Soszyński, M. K. Szymański, M. Kubiak, G. Pietrzyński, R. Poleski, Ł. Wyrzykowski, and K. Ulaczyk: 2011, 'V1309 Scorpii: merger of a contact binary'. *Astron. Astrophys.* **528**, A114.

Tylenda, R. and N. Soker: 2006, 'Eruptions of the V838 Mon type: stellar merger versus nuclear outburst models'. *Astron. Astrophys.* **451**(1), 223–236.

Ugliano, M., H.-T. Janka, A. Marek, and A. Arcones: 2012, 'Progenitor-explosion Connection and Remnant Birth Masses for Neutrino-driven Supernovae of Iron-core Progenitors'. *Astrophys. J.* **757**(1), 69.

Utrobin, V. P. and N. N. Chugai: 2019, 'Resolving the puzzle of type IIP SN 2016X'. *MNRAS* p. 2334.

Valenti, S., D. Sand, M. Stritzinger, D. A. Howell, I. Arcavi, C. McCully, M. J. Childress, E. Y. Hsiao, C. Contreras, N. Morrell, M. M. Phillips, M. Gromadzki, R. P. Kirshner, and G. H. Marion: 2015, 'Supernova 2013by: a Type IIL supernova with a IIP-like light-curve drop'. *MNRAS* **448**(3), 2608–2616.

Vlasis, A., L. Dessart, and E. Audit: 2016, 'Two-dimensional radiation hydrodynamics simulations of superluminous interacting supernovae of Type IIn'. *MNRAS* **458**(2), 1253–1266.

Webbink, R. F.: 1976, 'The evolution of low-mass close binary systems. I. The evolutionary fate of contact binaries.'. *Astrophys. J.* **209**, 829–845.

Webbink, R. F.: 1984, 'Double white dwarfs as progenitors of R Coronae Borealis stars and type I supernovae.'. *Astrophys. J.* **277**, 355–360.

Webbink, R. F.: 2008, 'Common Envelope Evolution Redux'. In: E. F. Milone, D. A. Leahy, and D. W. Hobill (eds.): *Astrophysics and Space Science Library*, Vol. 352. Springer, Berlin, Germany, p. 233.

Williams, S. C., D. Jones, P. Pessev, S. Geier, R. L. M. Corradi, I. M. Hook, M. J. Darnley, O. Pejcha, A. Núñez, S. Meingast, and S. Moran: 2020, 'AT 2019abn: multi-wavelength observations over the first 200 days'. *Astron. Astrophys.* **637**, A20.

Woosley, S. E.: 2017, 'Pulsational Pair-instability Supernovae'. *Astrophys. J.* **836**(2), 244.

Woosley, S. E., A. Heger, and T. A. Weaver: 2002, 'The evolution and explosion of massive stars'. *Reviews of Modern Physics* **74**(4), 1015–1071.

Woosley, S. E., T. Sukhbold, and H. T. Janka: 2020, 'The Birth Function for Black Holes and Neutron Stars in Close Binaries'. *Astrophys. J.* **896**(1), 56.

Xu, X.-J. and X.-D. Li: 2010, 'On the Binding Energy Parameter λ of Common Envelope Evolution'. *Astrophys. J.* **716**(1), 114–121.

Yamasaki, T. and S. Yamada: 2005, 'Effects of Rotation on the Revival of a Stalled Shock in Supernova Explosions'. *Astrophys. J.* **623**(2), 1000–1010.

Yamasaki, T. and S. Yamada: 2006, 'Standing Accretion Shocks in the Supernova Core: Effects of Convection and Realistic Equations of State'. *Astrophys. J.* **650**(1), 291–298.

Yamasaki, T. and S. Yamada: 2007, 'Stability of Accretion Flows with Stalled Shocks in Core-Collapse Supernovae'. *Astrophys. J.* **656**(2), 1019–1037.

Yaron, O., D. A. Perley, A. Gal-Yam, J. H. Groh, A. Horesh, E. O. Ofek, S. R. Kulkarni, J. Sollerman, C. Fransson, A. Rubin, P. Szabo, N. Sapir, F. Taddia, S. B. Cenko, S. Valenti, I. Arcavi, D. A. Howell, M. M. Kasliwal, P. M. Vreeswijk, D. Khazov, O. D. Fox, Y. Cao, O. Gnat, P. L. Kelly, P. E. Nugent, A. V. Filippenko, R. R. Laher, P. R. Wozniak, W. H. Lee, U. D. Rebbapragada, K. Maguire, M. Sullivan, and M. T. Soumagnac: 2017, 'Confined dense circumstellar material surrounding a regular type II supernova'. *Nature Physics* **13**(5), 510–517.

York, D. G., J. Adelman, J. Anderson, John E., S. F. Anderson, J. Annis, N. A. Bahcall, J. A. Bakken, R. Barkhouser, S. Bastian, E. Berman, W. N. Boroski, S. Bracker, C. Briegel, J. W. Briggs, J. Brinkmann, R. Brunner, S. Burles, L. Carey, M. A. Carr, F. J. Castander, B. Chen, P. L. Colestock, A. J. Connolly, J. H. Crocker, I. Csabai, P. C. Czarapata, J. E. Davis, M. Doi, T. Dombeck, D. Eisenstein, N. Ellman, B. R. Elms, M. L. Evans, X. Fan, G. R. Federwitz, L. Fiscelli, S. Friedman, J. A. Frieman, M. Fukugita, B. Gillespie, J. E. Gunn, V. K. Gurbani, E. de Haas, M. Haldeman, F. H. Harris, J. Hayes, T. M. Heckman, G. S. Hennessy, R. B. Hindsley, S. Holm, D. J. Holmgren, C.-h. Huang, C. Hull, D. Husby, S.-I. Ichikawa, T. Ichikawa, Ž. Ivezić, S. Kent, R. S. J. Kim, E. Kinney, M. Klaene, A. N. Kleinman, S. Kleinman, G. R. Knapp, J. Korienek, R. G. Kron, P. Z. Kunszt, D. Q. Lamb, B. Lee, R. F. Leger, S. Limmongkol, C. Lindenmeyer, D. C. Long, C. Loomis, J. Loveday, R. Lucinio, R. H. Lupton, B. MacKinnon, E. J. Mannery, P. M. Mantsch, B. Margon, P. McGehee, T. A. McKay, A. Meiksin, A. Merelli, D. G. Monet, J. A. Munn, V. K. Narayanan, T. Nash, E. Neilsen, R. Neswold, H. J. Newberg, R. C. Nichol, T. Nicinski, M. Nonino, N. Okada, S. Okamura, J. P. Ostriker, R. Owen, A. G. Pauls, J. Peoples, R. L. Peterson, D. Petravick, J. R. Pier, A. Pope, R. Pordes, A. Prosapio, R. Rechenmacher, T. R. Quinn, G. T. Richards, M. W. Richmond, C. H. Rivetta, C. M. Rockosi, K. Ruthmansdorfer, D. Sandford, D. J. Schlegel, D. P. Schneider, M. Sekiguchi, G. Sergey, K. Shimasaku, W. A. Siegmund, S. Smee, J. A. Smith, S. Snedden, R. Stone, C. Stoughton, M. A. Strauss, C. Stubbs, M. SubbaRao, A. S. Szalay, I. Szapudi, G. P. Szokoly, A. R. Thakar, C. Tremonti, D. L. Tucker, A. Uomoto, D. Vanden Berk, M. S. Vogeley, P. Waddell, S.-i. Wang, M. Watanabe, D. H. Weinberg, B. Yanny, N. Yasuda, and SDSS Collaboration: 2000, 'The Sloan Digital Sky Survey: Technical Summary'. *Astronom. J.* **120**(3), 1579–1587.

Zorotovic, M., M. R. Schreiber, B. T. Gänsicke, and A. Nebot Gómez-Morán: 2010, 'Post-common-envelope binaries from SDSS. IX: Constraining the common-envelope efficiency'. *Astron. Astrophys.* **520**, A86.

Chapter 3

Original Papers

3.1 Death of single stars

3.1.1 The landscape of the neutrino mechanism of core-collapse supernovae: neutron star and black hole mass functions, explosion energies, and nickel yields

Pejcha, O. and T. A. Thompson: 2015, 'The Landscape of the Neutrino Mechanism of Core-collapse Supernovae: Neutron Star and Black Hole Mass Functions, Explosion Energies, and Nickel Yields'. *Astrophys. J.* **801**(2), 90. doi:10.1088/0004-637X/801/2/90

3.1.2 A global model of the light curves and expansion velocities of Type II-Plateau supernovae

Pejcha, O. and J. L. Prieto: 2015a, 'A Global Model of The Light Curves and Expansion Velocities of Type II-plateau Supernovae'. *Astrophys. J.* **799**(2), 215. doi:10.1088/0004-637X/799/2/215

3.1.3 On the intrinsic diversity of Type II-Plateau supernovae

Pejcha, O. and J. L. Prieto: 2015b, 'On the Intrinsic Diversity of Type II-Plateau Supernovae'. *Astrophys. J.* **806**(2), 225. doi:10.1088/0004-637X/806/2/225

3.1.4 Supernova explosions interacting with aspherical circumstellar material: implications for light curves, spectral line profiles, and polarization

Kurfürst, P., O. Pejcha, and J. Krtička: 2020, 'Supernova explosions interacting with aspherical circumstellar material: implications for light curves, spectral line profiles, and polarization'. *Astron. Astrophys.* **642**, A214. doi:10.1051/0004-6361/202039073

3.2 Death of binary stars

3.2.1 Kinematics of mass-loss from the outer Lagrange point L2

Hubová, D. and O. Pejcha: 2019, 'Kinematics of mass-loss from the outer Lagrange point L2'. *MNRAS* **489**(1), 891–899. doi:10.1093/mnras/stz2208

3.2.2 Cool and luminous transients from mass-losing binary stars

Pejcha, O., B. D. Metzger, and K. Tomida: 2016a, 'Cool and luminous transients from mass-losing binary stars'. *MNRAS* **455**(4), 4351–4372. doi:10.1093/mnras/stv2592

3.2.3 Binary stellar mergers with marginally bound ejecta: excretion discs, inflated envelopes, outflows, and their luminous transients

Pejcha, O., B. D. Metzger, and K. Tomida: 2016b, 'Binary stellar mergers with marginally bound ejecta: excretion discs, inflated envelopes, outflows, and their luminous transients'. *MNRAS* **461**(3), 2527–2539. doi:10.1093/mnras/stw1481

3.2.4 Burying a binary: dynamical mass loss and a continuous optically thick outflow explain the candidate stellar merger V1309 Scorpii

Pejcha, O.: 2014, 'Burying a Binary: Dynamical Mass Loss and a Continuous Optically thick Outflow Explain the Candidate Stellar Merger V1309 Scorpii'. *Astrophys. J.* **788**(1), 22. doi:10.1088/0004-637X/788/1/22

3.2.5 Pre-explosion spiral mass loss of a binary star merger

Pejcha, O., B. D. Metzger, J. G. Tyles, and K. Tomida: 2017, 'Pre-explosion Spiral Mass Loss of a Binary Star Merger'. *Astrophys. J.* **850**(1), 59. doi:10.3847/1538-4357/aa95b9

3.2.6 Shock-powered light curves of luminous red novae as signatures of pre-dynamical mass-loss in stellar mergers

Metzger, B. D. and O. Pejcha: 2017, 'Shock-powered light curves of luminous red novae as signatures of pre-dynamical mass-loss in stellar mergers'. *MNRAS* **471**(3), 3200–3211. doi:10.1093/mnras/stx1768

3.2.7 On the triple-star origin of the planetary nebula Sh 2-71

Jones, D., O. Pejcha, and R. L. M. Corradi: 2019, 'On the triple-star origin of the planetary nebula Sh 2-71'. *MNRAS* **489**(2), 2195–2203. doi:10.1093/mnras/stz2293

3.2.8 The ASAS-SN catalogue of variable stars – IV. Periodic variables in the APOGEE survey

Pawlak, M., O. Pejcha, P. Jakubčík, T. Jayasinghe, C. S. Kochanek, K. Z. Stanek, B. J. Shappee, T. W. S. Holoien, T. A. Thompson, J. L. Prieto, S. Dong, J. V. Shields, G. Pojmanski, C. A. Britt, and D. Will: 2019, 'The ASAS-SN catalogue of variable stars - IV. Periodic variables in the APOGEE survey'. *MNRAS* **487**(4), 5932–5945. doi:10.1093/mnras/stz1681